
Masters Theses

Student Theses and Dissertations

Fall 2007

Characterization of coarse aggregate angularity using digital image processing

Gregory Allen Swift

Follow this and additional works at: https://scholarsmine.mst.edu/masters_theses



Part of the [Geological Engineering Commons](#)

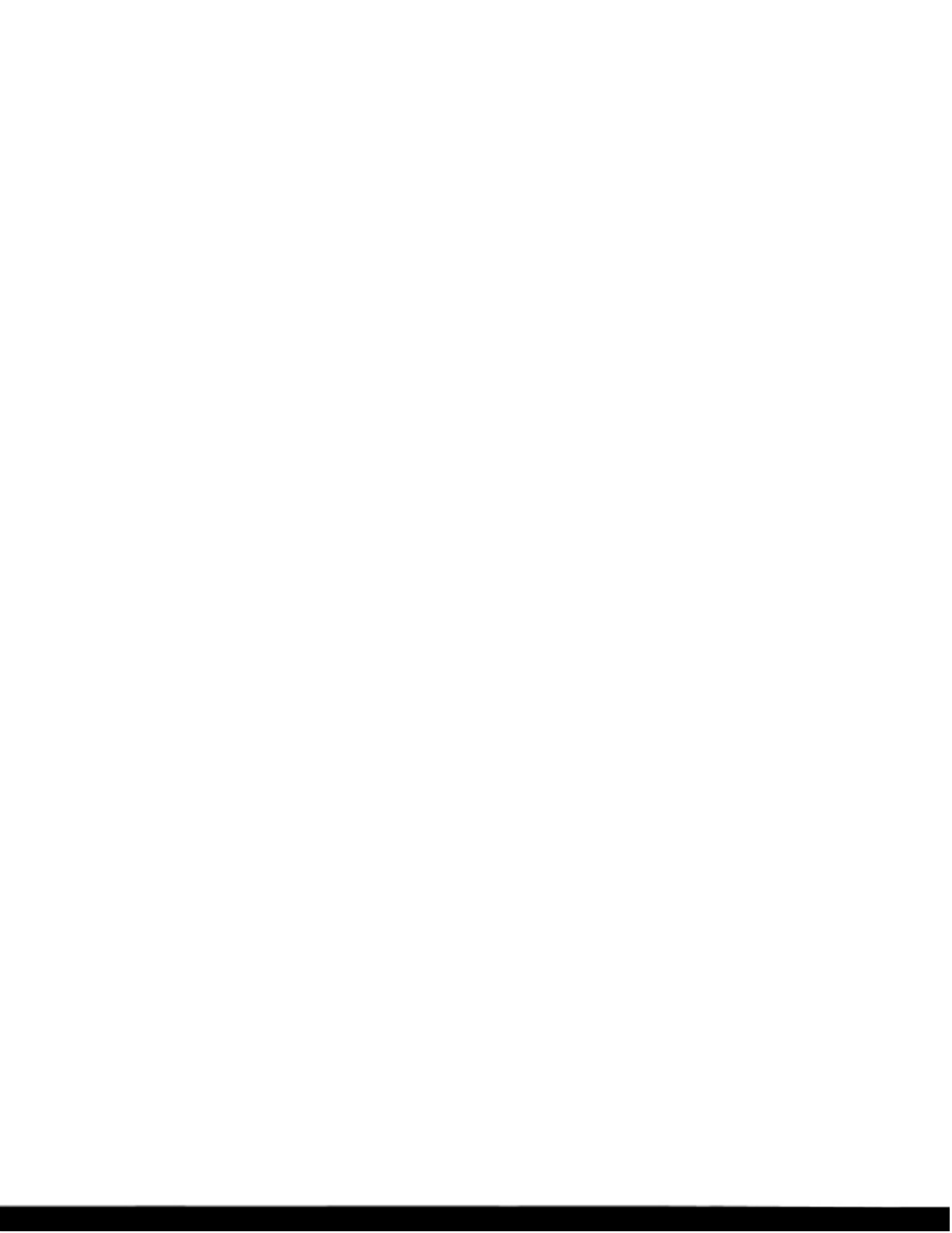
Department:

Recommended Citation

Swift, Gregory Allen, "Characterization of coarse aggregate angularity using digital image processing" (2007). *Masters Theses*. 4580.

https://scholarsmine.mst.edu/masters_theses/4580

This thesis is brought to you by Scholars' Mine, a service of the Missouri S&T Library and Learning Resources. This work is protected by U. S. Copyright Law. Unauthorized use including reproduction for redistribution requires the permission of the copyright holder. For more information, please contact scholarsmine@mst.edu.



CHARACTERIZATION OF COARSE AGGREGATE ANGULARITY
USING DIGITAL IMAGE PROCESSING

by

GREGORY ALLEN SWIFT

A THESIS

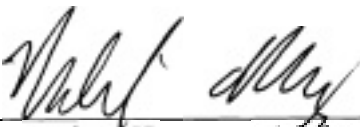
Presented to the Faculty of the Graduate School of the
UNIVERSITY OF MISSOURI-ROLLA

In Partial Fulfillment of the Requirements for the Degree

MASTER OF SCIENCE IN GEOLOGICAL ENGINEERING

2007

Approved by



Dr. Norbert H. Maerz, Advisor



Dr. Jeffery D. Cawfield



Dr. David N. Richardson



ABSTRACT

This thesis involves a comparative analysis study between three well established labor-intensive physical tests specified by ASTM and/or AASHTO standards for determining shape, angularity and texture of coarse aggregates and minimum average curve radius. Aggregate angularity of individual particles is defined by WipShape, a digital image-based system, as the Minimum Average Curve Radius.

Physical tests including Uncompacted Void Content, Index of Particle Shape and Texture (Compacted Voids), and Percentage of Fractured Particles, were conducted using several coarse aggregate samples, consisting of both river gravel and crushed rock. Minimum average curve radius measurements were obtained from the same aggregate samples using the WipShape imaging system and subsequently compared to physical testing results. A number of good correlations were found between Uncompacted Void Content, Compacted Voids and Minimum Average Curve Radius measurements. This implies that it may be possible to measure coarse aggregate angularity directly, discontinue the labor-intensive physical tests, and still generate similar results.

This paper is the result of a research project sponsored by the Transportation Research Board's National Cooperative Highway Research Program 4-30 that is intended to identify test methods, including digital imaging, for characterizing aggregate shape, texture, and angularity.

ACKNOWLEDGMENTS

First, I would like to thank my advisor, Dr. Norbert Maerz, for extending this opportunity to me. Without his patience and interest in my completion of this paper, I probably would not have finished. Second, I would like to thank the National Cooperative Highway Research IDEA Program for funding this research, and WipWare Inc. for providing a WipShape image analysis system and making modifications to the hardware and software. I would also like to thank the Missouri Department of Transportation (MoDOT) for their help and guidance, as well as the University of Missouri-Rolla Center for Infrastructure Engineering.

Further, I would like to thank my graduate committee, Dr. David Richardson and Dr. Jeffery Cawfield, along with Dr. Maerz, for taking the time and effort to serve on my committee and for their input and guidance. Finally, I would like to thank Joseph Molinaro for his help and especially Paula Cochran, for her guidance through the administrative process required in receiving my degree.

TABLE OF CONTENTS

	Page
ABSTRACT.....	iii
ACKNOWLEDGMENTS	iv
LIST OF ILLUSTRATIONS.....	viii
LIST OF TABLES.....	x
NOMENCLATURE	xi
SECTION	
1. INTRODUCTION.....	1
1.1. PROBLEM STATEMENT.....	1
1.2. BACKGROUND INFORMATION	1
1.3. SCOPE OF WORK.....	2
1.4. THESIS ORGANIZATION.....	3
2. LITERATURE REVIEW.....	5
2.1. IMPORTANCE OF AGGREGATE SHAPE	5
2.2. AGGREGATE SHAPE MEASUREMENT	6
2.3. STATE OF ART IN IMAGE-BASED MEASUREMENTS	7
2.3.1. Data Acquisition Procedures	7
2.3.2. Static Video Methods	7
2.3.3. Dynamic Video Methods.....	10
2.4. BENEFITS OF IMAGE-BASED MEASUREMENTS.....	15
3. WIPSHAPE IMAGING SYSTEM	17
3.1. HARDWARE DESCRIPTION	17
3.1.1. Black Mini-Conveyor Belt	17
3.1.2. Translucent Rotating Table	18
3.1.3. Imaging.....	19
3.2. SOFTWARE DESCRIPTION	19
3.2.1. Image Acquisition Loop.....	19
3.2.2. Measurements.....	20
3.2.3. Sizing.....	21

3.2.4. Aspect Ratio	21
3.2.5. Angularity.....	21
3.2.6. Data Output	24
3.2.7. Performance.....	24
4. PHYSICAL TESTING METHODS	25
4.1. PROCEDURE.....	25
4.1.1. Aggregate Samples Assembled for Testing	25
4.1.2. Control Samples	25
4.1.3. Bulk Samples.....	27
4.2. PHYSICAL LABORATORY TEST METHODS USED	27
4.2.1. Uncompacted Void Content of Coarse Aggregate.....	28
4.2.2. Index of Aggregate Particle Shape and Texture (Compacted Voids). ...	29
4.2.3. Fractured Particles in Coarse Aggregate	30
4.2.4. Bulk Specific Gravity of Coarse Aggregate.....	31
5. COMPARATIVE ANALYSIS OF PHYSICAL AND WIPSHAPE TESTING	32
5.1. PURPOSE OF COMPARATIVE ANALYSIS	32
5.2. CONTROL SAMPLE TESTING RESULTS.....	32
5.2.1. Uncompacted Void Content and Curve Radius	32
5.2.2. Compacted Voids and Curve Radius.....	33
5.2.3. Percentage of Fractured Particles and Curve Radius	33
5.3. ANALYSIS OF CONTROL SAMPLE RESULTS.....	34
5.4. BULK SAMPLE TESTING RESULTS	35
5.4.1. Uncompacted Void Content and Curve Radius	35
5.4.2. Compacted Voids (V10) and Curve Radius	36
5.4.3. Compacted Voids (V50) and Curve Radius	38
5.4.4. Percentage of Fractured Particles and Curve Radius	39
5.5. ANALYSIS OF BULK SAMPLE RESULTS.....	39
5.6. REPEATABILITY OF BULK SAMPLE TESTING.....	41
5.7. LIMITATIONS OF THE STUDY.....	43
6. CONCLUSIONS	44
6.1. CONCLUSIONS.....	44

6.2. RECOMMENDATIONS FOR FURTHER STUDY	46
APPENDICES	
A. CONTROL SAMPLE GRAPHS AND TESTING DATA.....	47
B. BULK SAMPLE GRAPHS AND TESTING DATA.....	53
C. AGGREGATE SAMPLE PHOTOGRAPHS	60
BIBLIOGRAPHY.....	65
VITA	70

LIST OF ILLUSTRATIONS

Figure	Page
2.1. Kou, Frost and Lai Method.....	8
2.2. Aggregate Imaging System.....	9
2.3. Laser-Based Aggregate Analysis System	10
2.4. French VDG-40 Videograder	10
2.5. Computer Particle Analyzer.....	11
2.6. Camsizer	12
2.7. Micrometrics OptiSizer System.....	13
2.8. Video Imaging System.....	13
2.9. Buffalo Wire Works System.....	14
2.10. University of Illinois Aggregate Image Analyzer.....	14
3.1. First Prototype of WipShape Imaging Device	17
3.2. Current Prototype of WipShape Imaging Device	18
3.3. WipShape Preparing to Analyze Image of a Rounded Particle	20
3.4. WipShape Minimum Average Curve Radius	22
3.5. WipShape Moving Curve Radius Measurements	23
3.6. WipShape Gaussian Smoothed Moving Curve Radii.....	24
3.7. WipShape Data Output	24
4.1. Control Samples.....	26
4.2. Uncompacted Void Content of Coarse Aggregate Apparatus	28
4.3. Index of Aggregate Particle Shape and Texture Molds.....	29
5.1. Uncompacted Void Content vs. Curve Radius for #4 and 3/8" Control Samples.....	32
5.2. Compacted Voids vs. Curve Radius for #4 Control Samples.....	33
5.3. Compacted Voids vs. Curve Radius for 3/8" Control Samples.....	33
5.4. Fractured Face Count vs. Curve Radius for #4 Control Samples	34
5.5. Fractured Face Count vs. Curve Radius for 3/8" Control Samples	34
5.6. Uncompacted Void Content vs. Curve Radius for #4 Bulk Samples	35
5.7. Uncompacted Void Content vs. Curve Radius for 3/8" Bulk Samples	36
5.8. Uncompacted Void Content vs. Curve Radius for 1/2" Bulk Samples	36

5.9. Compacted Voids (V10) vs. Curve Radius for #4 Bulk Samples.....	37
5.10. Compacted Voids (V10) vs. Curve Radius for 3/8” Bulk Samples.....	37
5.11. Compacted Voids (V10) vs. Curve Radius for 1/2” Bulk Samples.....	37
5.12. Compacted Voids (V50) vs. Curve Radius for #4 Bulk Samples.....	38
5.13. Compacted Voids (V50) vs. Curve Radius for 3/8” Bulk Samples.....	38
5.14. Compacted Voids (V50) vs. Curve Radius for 1/2” Bulk Samples.....	39
5.15. Uncompacted Void Content vs. Curve Radius for 1/2” Bulk Samples (without Missouri River Gravel Data).....	40

LIST OF TABLES

Table	Page
4.1. Aggregate Samples Assembled for Testing.....	25
4.2. Bulk Samples Used for Testing	27
5.1. Repeatability for Bulk Sample Testing.....	42

NOMENCLATURE

Symbol	Description
A	Oven Dry Weight of Sample
B	Weight of Saturated-Surface-Dry (SSD) Sample in Air
C	Weight of Saturated-Surface-Dry (SSD) Sample in Water
F	Mass of Fractured Particles with the Specified Number of Fractured Faces
$G_{sb,od}$	Bulk Specific Gravity, Oven Dry
M	Net Mass of Coarse Aggregate in Measure
M_{10}	Average Mass of Aggregate in Mold Compacted at 10 Drops per Layer
M_{50}	Average Mass of Aggregate in Mold Compacted at 50 Drops per Layer
N	Mass of Particles in the Non-Fractured Category
n	Number of Values in the Sample
P	Percent of Particles with the Specified Number of Fractured Faces
r	Repeatability
S	Bulk Dry Specific Gravity of the Aggregate Size Fraction
U	Percent of Uncompacted Voids in the Material
V	Volume of Cylindrical Mold, ml
V_{10}	Percent of Voids in Aggregate Compacted at 10 Drops per Layer
V_{50}	Percent of Voids in Aggregate Compacted at 50 Drops per Layer
σ	Single Operator Standard Deviation

1. INTRODUCTION

1.1. PROBLEM STATEMENT

Research was carried out to develop a method to measure coarse aggregate angularity of crushed stone and river gravel using image-based analysis, and compare to physically performed measurements, such as the Percent of Fractured Particles, Uncompacted Void Content and Index of Particle Shape (Compacted Voids).

The purpose of this research is to study the relationship between digital image processing and current physical testing methods for coarse aggregate shape and angularity to determine if correlations exist.

1.2. BACKGROUND INFORMATION

Crushed stone, gravel and sand encompass the bulk of the materials used in highway construction, whether for flexible asphalt, rigid concrete or unbound pavements. Careful selection of these materials ensures that the pavements will perform as designed, and that the pavements will not suffer from premature deformation.

Aggregates consequently must pass a stringent series of mechanical, chemical and physical tests in order to demonstrate that they will perform satisfactorily, and meet or exceed specifications. Examples of such mechanical tests include abrasion resistance, durability, and resistance to polishing. Chemical tests include sulfate soundness and organic content. Physical tests include aggregate gradations (determination of size distributions), aggregate shape, and angularity, sphericity, roundness and surface texture.

Rounded (as opposed to angular) aggregate particles are also a concern in the use of Hot Mix Asphalt (HMA) for highway construction. Rounded particles are associated with premature rutting (Masad et al., 2000). Rounded aggregate provides minimal aggregate interlock, and will easily roll over one another allowing movement within the mix, causing deep rutting in the pavement and affecting long-term performance (D'Angelo 1996). Increasing fine aggregate angularity will increase the VMA (voids in mineral aggregate) thereby reducing durability of the pavement (D'Angelo 1996).

The shape, angularity, and texture of aggregates affect several Portland cement concrete (PCC) properties, such as workability, water demand, and coarse aggregate-

mortar bond strength. Aggregates with smooth surface textures and more spherical shapes tend to require less mixing water and exhibit better workability than aggregates with rough surface textures and more angular shapes (NCHRP 2003). However, angular rough-textured aggregates have an increased surface area for bond to Portland cement paste and tend to produce better aggregate-mortar bond strengths when compared to similar sized rounded smooth-textured aggregates (ACI 1999).

The test procedures for many of the mechanical, chemical and physical tests have been well established and are specified, for example, by American Society for Testing and Materials (ASTM) standards, American Association of State Highway and Transportation Officials (AASHTO) standards, or Superior Performing Asphalt Pavements (Superpave) guidelines. In most cases the methods of testing is well accepted by the industry. However, physical testing, such as aggregate grading and aggregate shape has always been a time-consuming, tedious and labor-intensive process. Consequently these types of tests are often performed reluctantly and infrequently, resulting in test results that are perhaps not statistically representative.

New technologies, such as image processing, promise to increase the efficiency and productivity of the current labor-intensive tests. Imaging technologies for generating gradations as well as aggregate shape and related parameters are now commercially available.

Dr. Norbert H. Maerz, Assistant Professor at the University of Missouri-Rolla, has developed a prototype image analysis system for the measurement of flat and elongated and coarse aggregate angularity with the support of WipWare, Inc., a company specializing in image based granulometry. When fully developed, this system has the potential to replace time consuming subjective manual measurements for aggregate characterization and testing.

1.3. SCOPE OF WORK

This thesis involves a comparative analysis between well-established physically performed measurements for coarse aggregate and an image-based system. A thorough literature review was conducted, focusing on the importance of aggregate shape and how it is measured. In addition, state of art in image-based aggregate measurement was

reviewed along with the impacts and difficulties of an image-based methodology. Physical testing, consisting of Uncompacted Void Content, Index of Particle Shape and Texture (Compacted Voids), and Percent of Fractured Particles (fractured face or crush counts), was performed on aggregate control samples prior to testing on bulk aggregate samples. All aggregate samples were then tested with the WipShape imaging system to obtain Minimum Average Curve Radius measurement data. Finally, the results of physical testing and Minimum Average Curve Radius measurements were analyzed to determine if correlations exist between the different methods.

1.4. THESIS ORGANIZATION

This thesis is broken down into six sections: Introduction, Literature Review, WipShape Imaging System, Physical Testing Methods, Comparative Analysis of Physical and WipShape Testing and Conclusions. The Introduction section includes information about the problem statement and scope of work. The Literature Review section discusses aggregate shape, angularity, and surface texture and how they affect pavement performance. It also discusses currently performed labor-intensive physical measurements. Finally, the state of art for image-based measurements is presented with potential impacts and difficulties using an image-based methodology.

The third section, WipShape Imaging System, focuses on the coarse aggregate image-based measurement system used in this study. A hardware description of the first and final prototypes is presented, describing the process of transporting individual pieces of aggregate to the cameras so they can be imaged. A software description is also presented, which discusses the operations such as image acquisition, measurements, and data output performed when an individual piece of aggregate is transported to the cameras.

The Physical Testing Methods section focuses on procedures for three well established labor-intensive physical tests specified by American Society of Testing and Materials (ASTM) standards and/or American Association of State Highway and Transportation Officials (AASHTO) standards. It also focuses on control and bulk aggregate samples used for comparative analyses between physical and WipShape (Minimum Average Curve Radius) testing methods.

The Comparative Analysis of Physical and WipShape Testing section focuses on the results and analyses from the physical and digital image testing. Data that were produced by both types of testing were compared and analyzed using spreadsheets. Correlations between physical and digital image testing results were examined to determine if Minimum Average Curve Radius is a good measure of aggregate shape. Finally, the Conclusions section summarizes the major conclusions developed from this study and makes recommendations for future work. Appendices A and B includes graphs and testing data from physical and WipShape testing while photographs of the aggregates used in this study are presented in Appendix C.

2. LITERATURE REVIEW

2.1. IMPORTANCE OF AGGREGATE SHAPE

Aggregate particle shape, angularity, and surface texture are known to affect the performance and durability of flexible asphalt pavements, rigid concrete, and to a lesser extent unbound pavements (Benson 1968, Britton 1968, Kalcheff and Tunnicliff 1982), which has been known for some time. Flat or elongated aggregates are thought to break down during the asphalt emplacement process resulting in incorrect gradations (Buchanan, 2000), and flat aggregates tend to lie flat, imparting anisotropic properties (weakness) to the finished product (Maerz and Lusher, 2001). When dealing with Hot Mix Asphalt (HMA) design, aggregate must provide enough shear strength to resist repeated load applications (Asphalt Institute 1996). If the aggregate mass is subjected to excessive loads, a shear plane develops that can result in permanent deformation. Aggregate shear strength is critically important in HMA because it provides the mixture's primary rutting resistance (Asphalt Institute 1996). Cubical, rough-textured aggregates provide more resistance to movement in the stone skeleton than rounded, smooth-textured aggregates (Asphalt Institute 1996).

This understanding is reflected in the new Superpave (Superior Performing Asphalt Pavements) guidelines developed as a product of the Strategic Highway Research Program (SHRP). D'Angelo (1996) summarized these concepts:

1. It is well known that the stability of pavement mixtures increases with increased angularity of the coarse aggregate materials comprising the 80-85% fraction of flexible asphalt pavements. Rounded aggregate provides minimal aggregate interlock, and will easily roll over one another allowing movement with the mix, and deep rutting in the long term performance.
2. Increasing fine aggregate angularity will increase the VMA (voids in mineral aggregate) thereby reducing durability of the pavement.
3. Flat and elongated particles will tend to lie flat during the compaction phase of emplacement, resulting in anisotropic properties and slip planes, and reducing aggregate interlock.

4. Flat and elongated particles will tend to break during the compaction phase of emplacement, changing the design gradation characteristics of the aggregate part of the mix. In some cases the deterioration could drive the gradation curve into the so-called “restricted zone”, a zone through which the gradation is not allowed to pass.

2.2. AGGREGATE SHAPE MEASUREMENT

There are three independent measures that can be considered as indicators of particle shape. These are aspect ratio (form, sphericity), roundness (angularity), and surface texture (particle texture) (Masad, et al. 2001). The available measurement methods of coarse aggregate shape, angularity, and texture are few; mostly indirect measurements and results are uneven at best.

Aggregate shape is nominally defined by the descriptive terms sphericity (aspect ratio) and roundness (Barrett 1980, Smith and Collis 2001, Wadell 1932), which are intuitively obvious but difficult to quantify. Historically, only aspect ratio and roundness have been considered to be indicators of shape (Pettijohn 1949, Krumbein and Sloss 1951). Presently, the test that best quantifies sphericity and roundness is the Percentage of Fractured Particles in coarse aggregate, or Fractured Face Count (National Stone, 1990). This test can determine whether rounded aggregate pieces have been sufficiently crushed as to present at least two good fractured faces. However, this test is completely manual, time consuming, labor intensive and subjective.

Two more tests attempt to use a presumed correlation between void ratio and shape, one uncompacted (Uncompacted Void Content of Coarse Aggregate, AASHTO Designation TP56-99), and one compacted (Index of Aggregate Particle Shape and Texture, ASTM D3398-00). There is also a fine aggregate equivalent test (Uncompacted Void Content of Fine Aggregate, ASTM C1252, and AASHTO TP33). The uncompacted method describes the determination of void content of a sample of coarse aggregate. When measured on any aggregate of a known grading, void content provides an indication of the aggregate’s angularity, sphericity, and surface texture compared with other coarse aggregates tested in the same grading (AASHTO Designation TP56-99). The compacted (or Index) method covers the determination of the particle index of

aggregate as an overall measure of particle shape and texture characteristics (ASTM D3398-00).

Aggregate texture, nominally defined as roughness (smooth-glassy vs rough-sandpaper; National Stone, 1990), is also intuitively obvious but difficult to quantify. These above mentioned void tests are also often quoted as “measuring texture”, especially the Index of Aggregate Particle Shape and Texture procedure. The connection between these tests and surface texture has to our knowledge not been established.

Texture requires measurement at a different scale of observation and is not normally directly tested for at the aggregate level. However, tests for frictional properties of final pavements are common and include various polishing wheel and pendulum tests.

2.3. STATE OF ART IN IMAGE-BASED MEASUREMENTS

Data acquisition procedures, three-dimensional static and dynamic video methods, and videograders have been developed with the intention of replacing some or all of the physical/manual tests discussed with imaging devices (Masad, et al., 2000, Masad, et al., 2001).

2.3.1. Data Acquisition Procedures. Barksdale, et al. (1991) researched the possibility of using modern data acquisition procedures to measure aggregate. Although they did not have a definite method or designed apparatus to measure aggregate they concluded that with a relatively low-cost digitizer and microcomputer, it is possible to acquire large quantities of accurate data rapidly. With the assistance of AutoCAD and a spreadsheet program, they were able to acquire and process large amounts of data and make possible easy presentation and interpretation of data describing shape, surface area, and roughness.

2.3.2. Static Video Methods. Kuo, et al. (1996), (1998), and Frost, et al. (1996) developed a method to analyze the morphological characteristics of coarse aggregate using a three dimensional image analysis process. They demonstrated that the method could efficiently and accurately measure flatness and elongation of aggregate. Although this method can clearly measure aggregate three dimensionally, there is still some significant amount of manual work that has to be applied because the aggregate in this method is measured on plexiglass holders that have to be reloaded with new aggregate

particles each time as illustrated in Figure 2.1. The method that Kuo and his colleagues studied is a large step in the process of image analysis of coarse aggregate, because he was able to eliminate the subjectivity that the manual testing procedure created.

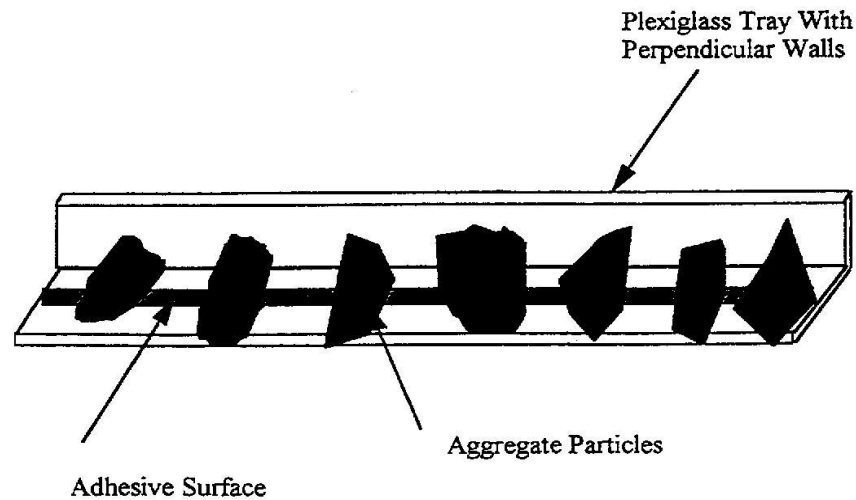


Figure 2.1. Kuo, Frost and Lai Method

Another problem that could be faced with the plexiglass holders is that the cameras look at the particles at different angles and different lighting conditions on the outer ends of the tray than the particles in the center of the tray directly in line with the cameras. Brzezicki and Kasperkiewicz (1999) had a similar idea as Kuo and his colleagues as to how to measure aggregate, except they measured the shadows along with the aggregate particle at perpendicular projections, enabling three-dimensional characteristics to be measured. This approach allowed them to evaluate the three main dimensions (length, width, and height) of the particle. They concluded that this method would be very effective for measurements of aggregate shape and that with the appropriate hardware this method could be modified to measure aggregate on a moving conveyor belt. They also agreed that the implementation of using an image analysis program would help improve quality control of aggregate production.

The Aggregate Imaging System operates based on two modules. The first module analyzes fine aggregate and the second module analyzes coarse aggregate using a video

camera and microscope (Fletcher, et al. 2002, Masad 2003). Fine aggregates are analyzed for shape and angularity, while coarse aggregates are analyzed for shape, angularity and texture. Shape is quantified by two dimensional projections plus the depth of the particles, which is determined by the microscope. The imaging system uses 56 particles when analyzing coarse aggregate and uses a few grams when analyzing fine aggregate. Figure 2.2 shows the Aggregate Imaging System analyzing coarse aggregate.

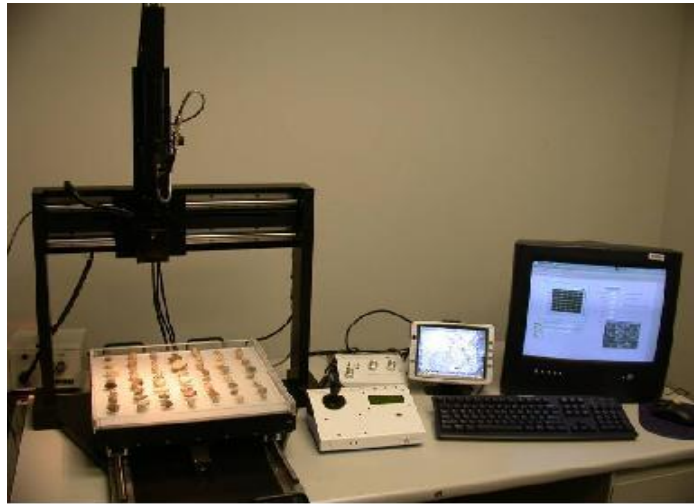


Figure 2.2. Aggregate Imaging System

Another static method is the Laser-Based Aggregate Analysis System. This system was developed at the University of Texas-Austin to characterize size and shape parameters of coarse aggregates (Kim, et al. 2001, Kim, et al. 2002). A laser scanner passes over an aggregate sample scattered on a platform. The three-dimensional scanner data are transformed into gray-scale digital images. Gray-scale pixel values determine the height of each datum point and the heights are used to calculate shape, angularity and texture parameters. One disadvantage of this system is it uses the same scan to analyze aggregates with different sizes. Figure 2.3 illustrates the components of the Laser-Based Aggregate Analysis System.

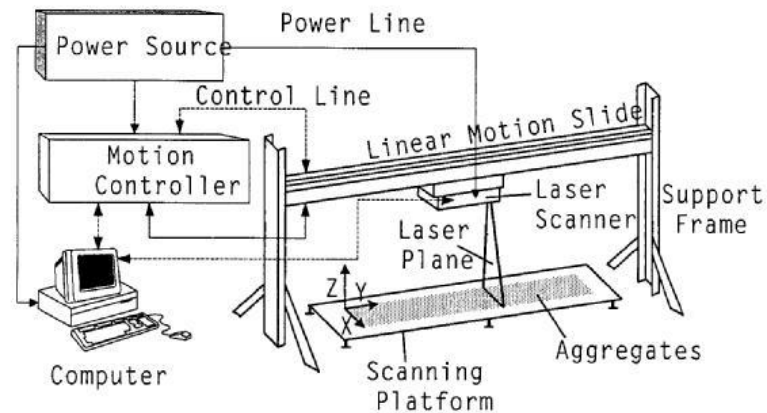


Figure 2.3. Laser-Based Aggregate Analysis System

2.3.3. Dynamic Video Methods. Another method developed to measure aggregate shape and size is the VDG-40 Videograder shown in Figure 2.4. Prowell and Weingart evaluated the precision of the VDG-40 in measuring flat and elongated particles (Prowell and Weingart 1999, Weingart and Prowell 1998/1999). The VDG-40 is argued to have been developed originally for granulometry and not for particle shape measurement (Maerz and Lusher 2001).



Figure 2.4. French VDG-40 Videograder

In determining the viability of the VDG-40 being able to accurately measure the percent of flat and elongated particles in accordance with ASTM D4791 there was too much variability seen. The most apparent reason for the high amount of variability in the analysis is because Prowell and Weingart attempted to correlate the slenderness ratio that was measured by the apparatus and translate the French test method (which was the basis of their test method) to work in accordance with the ASTM D4791 by incorporating a Shape Class Average Ratio (SCAR) formula (Prowell and Weingart 1999). This formula assumes that on average, a particle between two ratios would have dimensions equal to the average of those two ratios. Since a strong correlation between the VDG-40 and ASTM D4791 was not able to be determined, this testing device has not seen efficient use in the U.S. along with its high initial capital cost (Weingart and Prowell 1998/1999).

The Computer Particle Analyzer, shown in Figure 2.5, is similar to the VDG-40 Videograder, as it uses a charge-coupled device (CCD) camera to image and evaluate each particle as it falls in front of a backlight. The finalized data is stored and sorted into 250 classes, which amounts to an analysis equivalent to 250 sieve measurements. The information is presented in sieve size fractions or shape calculations (Browne, et al. 2001, Tyler, 2001). According to the manufactures, this device has been continually testing throughout the 1990's and the repeatability of the machine is very good. However, the Computer Particle Analyzer does not address angularity or surface texture and assumes an idealized particle shape to provide information on shape.



Figure 2.5. Computer Particle Analyzer

The Camsizer device consists of two optically matched digital cameras that are used to capture images of fine and coarse aggregates at different resolutions. Individual particles exit a hopper to a feed chamber and fall between a light source and the cameras. This system, manufactured by Retsch Technology, is commercially available and measures aggregate form, sphericity, symmetry, and length to breadth. The Camsizer device, with its optically matched digital cameras, is shown in Figure 2.6.

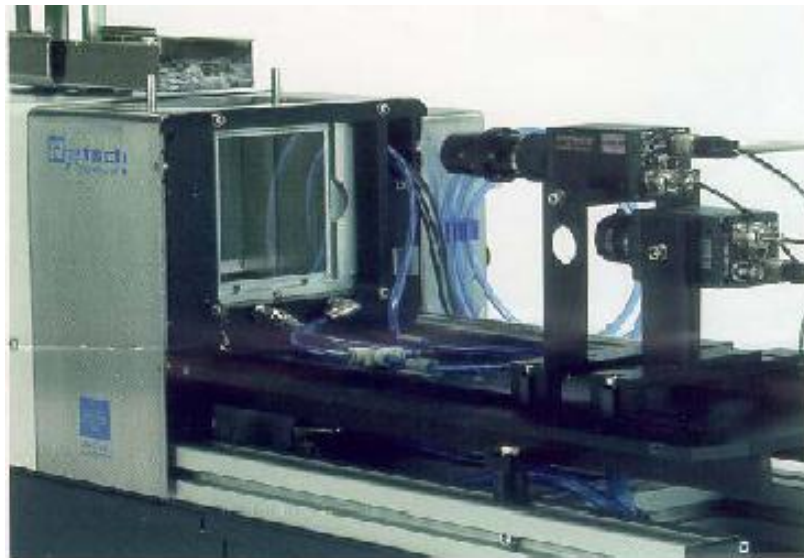


Figure 2.6. Camsizer

The Micrometrics OptiSizer and Video Imaging System are similar to the VDG-40 Videograder. Both systems use a line-scan CCD camera that evaluates particles as they fall in front of backlights (Browne, et al. 2001). Both also assume an idealized particle shape to provide information on gradation and shape. The only differences between the two systems identified in the literature are the physical configurations and analysis and data reporting with the custom software packages. The Micrometrics OptiSizer is shown in Figure 2.7 and the Video Imaging System is shown in Figure 2.8.



Figure 2.7. Micrometrics OptiSizer System



Figure 2.8. Video Imaging System

Buffalo Wire Works system was developed at the University of Tennessee. Using similar principles as the VDG-40 Videograder and Camsizer, the system utilizes one line-scan CCD camera to image and evaluate particles as they fall in front of a backlight, which provides information about gradation and shape. Two separate devices, one large and one small, were developed for a laboratory environment and both use the same analysis concept for coarse and fine aggregates (Browne, et al. 2001). However, the Buffalo Wire Works system does not address angularity or surface texture. The Buffalo Wire Works system, large device, is shown Figure 2.9.



Figure 2.9. Buffalo Wire Works System

The University of Illinois Aggregate Image Analyzer was initially developed by Rao and Tutumluer (2000) using three cameras at orthogonal views to measure the volume of an aggregate as well as the aspect ratios. An illustration of the Aggregate Image Analyzer is shown in Figure 2.10.

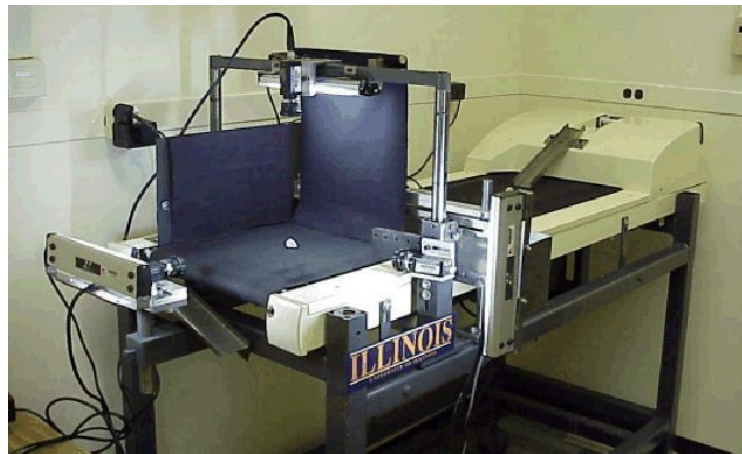


Figure 2.10. University of Illinois Aggregate Image Analyzer

Rao and Tutumluer created a video imaging system with a similar setup used by Kuo, et al. (1996) to perform digital analysis of aggregates. On their sensitivity study,

they were experiencing problems with user selected parameters (Tutumluer, et al. 1999). Also, problems were encountered with the aggregate laying on plexiglass trays and the cameras looking at each aggregate particle at a different angle, which resulted in variable lighting conditions on each particle due to shadows. In addition, problems were encountered properly focusing the cameras on each aggregate particle.

Currently, the Aggregate Image System uses three orthogonally positioned cameras to capture three-dimensional views of each aggregate as it moves along a conveyor belt. It has the capabilities to determine the volume, flat and elongated ratio, sieve size, angularity and surface texture (Rao, et al. 2002). The most recent research work found in the literature was the addition of a module to measure surface texture characteristics of coarse aggregates by using erosion and dilation techniques (Rao, et al. 2003). According to the literature, the system provides promising results in the area of digital image analysis. However, one inconvenience is that the apparatus is large and cumbersome.

WipShape imaging system, a method developed by Dr. Maerz at the University of Missouri-Rolla, is used in this study and has been described in earlier papers by Maerz, et al. (1999 and 2001) (Maerz 1998). This imaging system is presented in greater detail in Section 3.

2.4. BENEFITS OF IMAGE-BASED MEASUREMENTS

The potential impact of this technology is substantial. Using the imaging methodology, an analysis will be completely automated, requiring only that the operator load the feed hopper with an aggregate material that has been cut off at the #4 sieve size, start the machine, and read the results a few minutes later. The following impacts of a successful image based methodology are numerous:

1. Test results, removed from human subjectivity, have the potential to be much more reliable. No longer will the test results vary between operators, or vary based on the disposition of an operator.

2. A greater number of tests will be performed. Faster testing, and the low per unit cost of incremental tests, will result in an increased amount of tests being conducted, allowing better and more statistically valid characterization.
3. Run time adjustments to crushing, screening and other processing equipment will be possible. Because the analysis is quick, a significant reduction of off-specification material can be achieved, and there will be less incentive to pass off-specification material.
4. There will be a lower burden on operators and testing agencies, resulting from lower per sample testing costs.

However, the following points reveal that there are also difficulties with image based measurement methodologies:

1. The capital costs of imaging equipment will be much higher.
2. Inherent small to significant differences in measurement results can be expected, because of the differences between imaging and physical testing techniques.
3. Industry and regulatory resistance can be expected to any new technology that does not give exactly the same results as the “older” manual measurements, even if the “older” measurements are less accurate.

3. WIPSHAPE IMAGING SYSTEM

3.1. HARDWARE DESCRIPTION

Imaging systems require the individual aggregate pieces be transported to where they can be imaged by the camera, and then moved out of the way so that others can be imaged. Furthermore, for the purpose of three-dimensional imaging, pieces must be imaged individually so that the same piece can be unambiguously identified in both views. Two prototype devices have been designed; a black mini-conveyor belt and a translucent rotating table.

3.1.1. Black Mini-Conveyor Belt. The first prototype sample presentation used a black belt to create a contrast between the sample and background. It featured a vibrating feeder, black transport belt, and chute discharge. A black backdrop was added with small lamps used for variable intensity and variable angle illumination. Two orthogonal cameras, plan and profile view, are mounted on extension arms. The first WipShape prototype is shown in Figure 3.1.



Figure 3.1. First Prototype of WipShape Imaging Device

The black belt and backdrop serve to create a contrast between the sample and the background to aid in the identification of block edges. Small 4 watt lamps on flexible mounts serve to give directed variable angle lighting to increase the contrast between the

aggregate piece and the backdrop, and to avoid glare from direct reflections. Cameras are mounted on extension arms, and take plan and profile images.

The belt has an operational speed of about 0.055 meters per second (m/s) and a maximum speed of 0.18 m/s. The vibrating feeder is adjustable to increase or decrease vibration. The vibration level is typically set in conjunction with the belt speed so that there is a least a 2-inch separation of particles (aggregate pieces) when they are placed on the belt.

This device works well for light colored aggregates, but it is difficult to maintain the contrast with darker or mottled aggregates due to the black belt reflecting a significant amount of light.

3.1.2. Translucent Rotating Table. The current WipShape prototype uses a translucent rotating table to create contrast by backlighting and imaging a silhouette. It features a vibrating feeder, circular translucent transport table, and a rotating brush for discharge. Fiber optic backlighting is used for variable illumination. Two orthogonal cameras (plan and profile views) are mounted on extension arms. The current WipShape prototype, with a plan view (left) and profile view (right) of the aggregate, is shown in Figure 3.2.

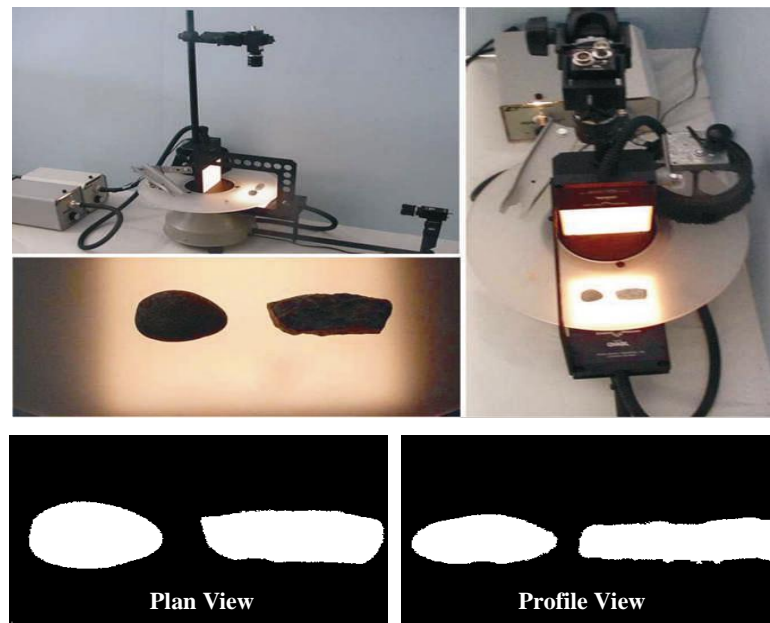


Figure 3.2. Current Prototype of WipShape Imaging Device

The table has an operational speed (at the center of the image) of approximately 0.080 m/s or 10.9 revolutions per minute (rpm) and a maximum speed of 0.15 m/s or 20.0 rpm. The vibrating feeder is the same as for the black mini-conveyor.

This device works well for all aggregates, however very light colored aggregates are sometimes difficult to silhouette completely due to cross-contamination of light. The light that silhouettes the fragment (aggregate) in the profile view also reflects light off the fragment in plan view.

3.1.3. Imaging. The cameras used for this application are a pair of Sentech STC-1000 progressive scan (non-interlaced), double speed cameras. The cameras are synchronized with each other, so they are imaging simultaneously at 60 frames per second.

The digitization board is an Imaging Source DFG-BWI. This board simultaneously digitizes images from both cameras, and provides the power and triggers to the cameras. On-board look-up tables allow real-time thresholding. This produces the binary image required (2 bits per pixel), and reduces the bandwidth required for transferring images.

3.2. SOFTWARE DESCRIPTION

The software application is developed as a *Windows*® application under *Using Visual c++*® and consists of a software trigger to determine if a block is present in both views, a particle identification routine, and measures on the two views of the particle.

3.2.1. Image Acquisition Loop. Image acquisition is facilitated by a capture software development kit provided by the manufacturer of the digitization board. A dual binary image is captured and brought to the image buffer in the application. The acquisition board provides for lookup tables, which allow real-time thresholding; a binary (black and white, 1-bit per pixel) image is transferred from the acquisition board to the host buffer.

Image acquisition is a continuous loop, in real time. A software trigger (triggered by the presence of a block under the vertical and horizontal search lines as shown in Figure 3.3) looking for five or more contiguous white pixels along the trigger lines, determines that a block is present in both views. If a block is found, it is analyzed. If no block is found, the next set of images is acquired. Figure 3.3 illustrates a captured dual

binary image of a rounded particle set to be analyzed, with vertical and horizontal parallel lines as trigger searches.

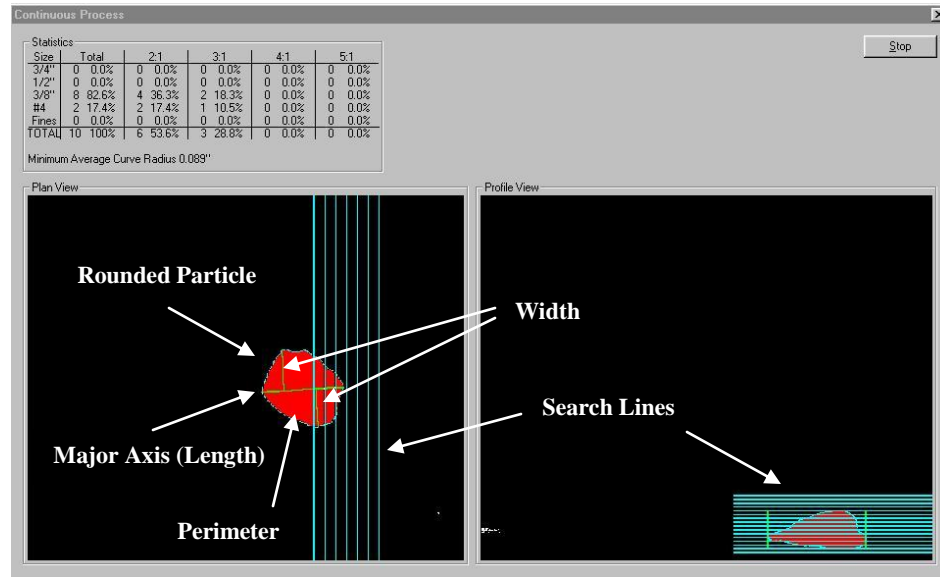


Figure 3.3. WipShape Preparing to Analyze Image of a Rounded Particle

3.2.2. Measurements. Using the binary image in Figure 3.3, the following operations are executed.

1. A perimeter walk creates an array of x-y coordinates defining the outline of each view of the block. The perimeter is painted yellow and placed into a vector array of perimeter coordinates.
2. A recursive pixel filling (paint) routine calculates the profile surface area of each view of the block. The area is painted red.
3. In the plan view, using the perimeter array, the longest dimension (major axis, length) is identified and measured as the length of the aggregate. The line between two points that are the farthest apart are defined as the maximum dimension (length). This line is painted green.
4. In the plan view, the longest half-width on each side of and perpendicular to the major axis is identified and measured. The perpendicular distance is measured between each point on one side of the particle and the line

defining the length, for both sides. Adding both lengths together gives the width of the aggregate. Both lines are painted green.

5. In the profile view, using the perimeter array, the maximum height of the particle is identified and measured by determining the difference in length between the highest point and lowest parts of the profile.
6. If the maximum dimension is not greater than the intermediate dimension, or the intermediate dimension is not greater than the minimum dimension, the measurements are re-ordered.

3.2.3. Sizing. The size of the aggregate is taken to be the width of the particle. This is to provide compatibility with screening results (It is primarily the width that governs the minimum screen size that a particle can pass through). An empirical calibration factor is used to match screening size measurements. It was experimentally determined that the best estimate of particle volume could be determined by equation 1.

$$[\text{volume} = \text{length} \times \text{width} \times \text{height} \times 0.8] \quad (1)$$

This reflects the fact that statistically, the typical particle observed occupies about 80 percent of the volume of a rectangular parallelepiped of the same length, width, and height. While this relationship will vary depending on the degree of rounding of the edges, it is irrelevant in the final analysis as results are normalized by weight percent.

3.2.4. Aspect Ratio. Aspect ratio is easy to visualize and easy to measure in a regular-shaped particle. The “box principle” uses the idea of fitting a three-dimensional box around the aggregate piece and recording the size of the box in terms of length, width and height. The aspect ratio is determined by dividing the maximum dimension (length) by the minimum dimension (height). Particles are classified as being greater than 5:1, 4:1, 3:1, 2:1 or 1:1.

3.2.5. Angularity. Many shape measurements are presented in the literature such as sphericity, roundness, Fourier spectra of profiles and fractal dimension of profiles (Franklin 1996a,b). Janoo (1998) described several methods of characterizing shape such as degree of angularity, roundness and roughness indexes. These were implemented with

no apparent good correlation to actual shape. Next, chord length distributions were measures, without any more success. Finally, Krumbein (1940), Pettijohn (1949), and Krumbein and Sloss (1951) approach was tried, which consists of using inscribed circles fitted into the corners (vertices) of the projection of the particles, and then attempting to measure the radius of curvature. This is the technique used for the imaging system.

WipShape aggregate angularity is defined as the Minimum Average Curve Radius of the individual particles. Minimum Average Curve Radius calculations applied to rounded and angular aggregate particles are illustrated in Figure 3.4. The aggregate profiles, with inscribed curve radii that are measured by an algorithm, are shown below the individual particles.

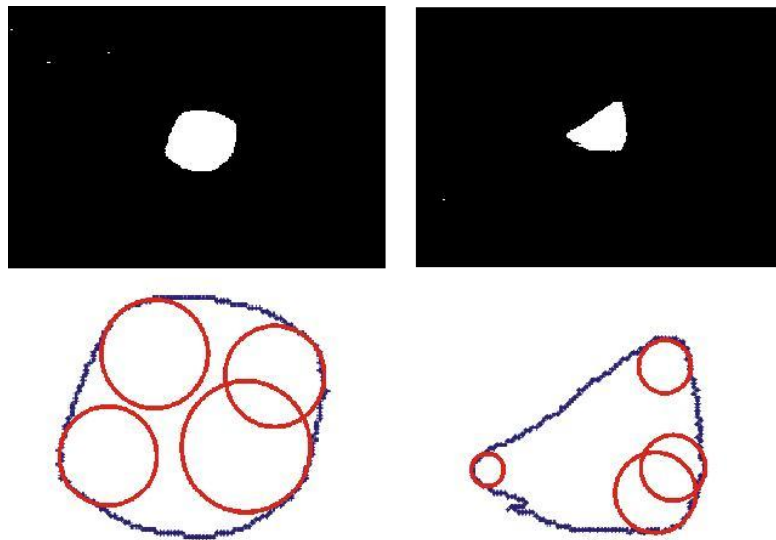


Figure 3.4. WipShape Minimum Average Curve Radius

The angularity or Minimum Average Curve Radius for each particle is calculated by WipShape with the following steps:

1. From the perimeter array, the radius of a circle containing three points on the profile is calculated. Each point is separated by ten pixels along the perimeter (a ten pixel separation was determined to be small enough to be sensitive to small curves, but large enough to be unaffected by the noise and aliasing along the

perimeter). An instantaneous curve radius is determined for each point on the profile in this manner, creating an array of curve radii as shown in Figure 3.5.

2. The array of curve radii values are smoothed by a moving average filter. A five-point Gaussian low pass filter is used.
3. The array of smoothed curve radii is examined to find local minima in the curve radius function.
4. A test is performed to ensure that a corner of the aggregate piece does not result in more than one local minima.
5. The list of local minimum curve radii is ordered from smallest to largest.
6. The four smallest curve radii are averaged to produce the Minimum Average Curve Radius of the individual particle.

WipShape moving curve radius measurements around profiles of corresponding aggregate particles are illustrated in Figure 3.5. The Gaussian smoothed moving curve radii for the rounded particle in Figure 3.5 are shown in Figure 3.6.

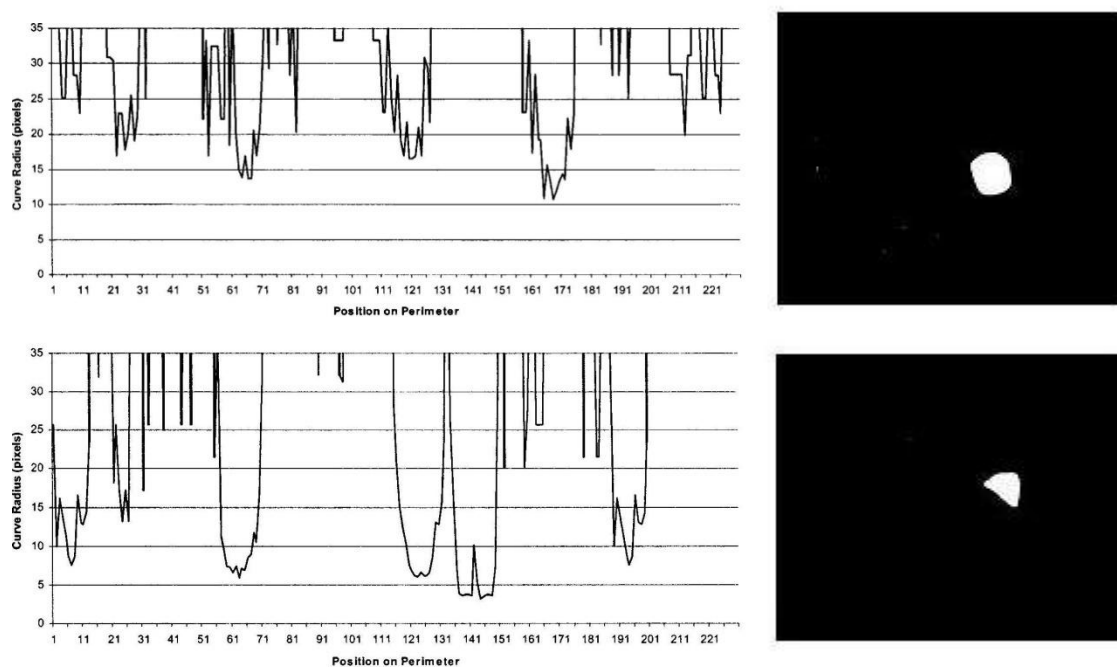


Figure 3.5. WipShape Moving Curve Radius Measurements

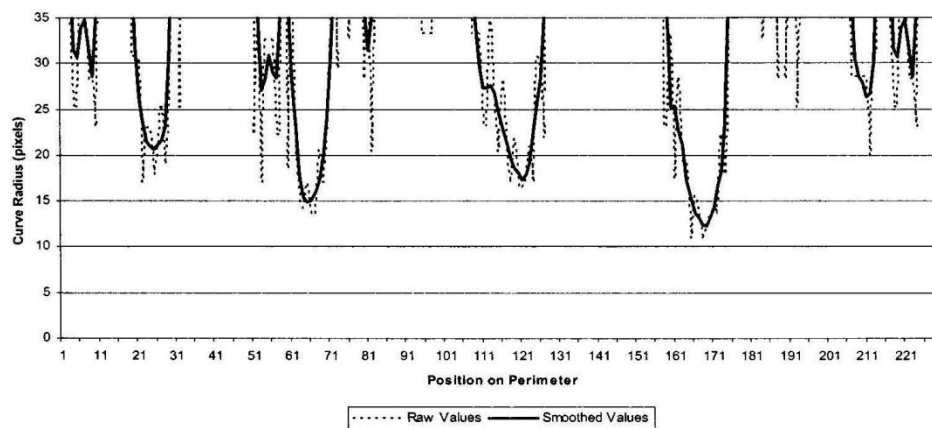


Figure 3.6. WipShape Gaussian Smoothed Moving Curve Radii

3.2.6. Data Output. Data are output as a chart of aspect ratio verses size retained as shown in Figure 3.7. In each category, the numbers of particles found are listed as well as the weight percent. On the bottom, the Minimum Average Curve Radius is provided in inches.

WipShape Analysis									
Size	Total		2:1		3:1		4:1		5:1
3/4"	10 4.6%		8 3.4%		6 1.9%		2 0.6%		1 0.3%
1/2"	248 89.8%		167 58.7%		51 14.9%		16 3.8%		5 0.8%
3/8"	23 5.5%		13 3.1%		1 0.2%		0 0.0%		0 0.0%
#4	0 0.0%		0 0.0%		0 0.0%		0 0.0%		0 0.0%
Fines	0 0.0%		0 0.0%		0 0.0%		0 0.0%		0 0.0%
TOTAL	281 100%		188 65.2%		58 17.0%		18 4.4%		6 1.1%

Minimum Average Curve Radius 0.096"

Figure 3.7. WipShape Data Output

3.2.7. Performance. A sample of 100 pieces of aggregate takes less than two minutes to process using the imaging system. This compares to more than fifteen minutes for a typical voids test, not counting calculations and report preparation.

4. PHYSICAL TESTING METHODS

4.1. PROCEDURE

Aggregate samples were assembled from several different geologic formations exhibiting various ranges of particle shape, angularity and surface texture. The samples within each formation were separated into various individual sieve sizes, washed and dried prior to physical and WipShape testing. In the Software Description section for the WipShape Imaging System, it has been shown that Minimum Average Curve Radius is a function of size by using inscribed circles fitted into the corners of the projection of the aggregate, and then measuring the radius of curvature. Therefore, individual aggregate sizes were analyzed separately. Simple control samples were assembled to evaluate WipShape algorithms prior to testing the bulk samples.

4.1.1. Aggregate Samples Assembled for Testing. Sample bags of crushed stone and uncrushed river gravel were acquired through the efforts of the Missouri Department of Transportation (MoDOT) from a few quarries throughout the state. Information regarding the types of aggregate obtained and their sources are presented in Table 4.1.

Table 4.1. Aggregate Samples Assembled for Testing

Samples	Geologic Formation	Source/Location	Crushed (Yes/No)
Canadian Limestone	Bobcaygeon	Brechin Quarry/Ontario, Canada	Yes
Higginsville Limestone	Higginsville	Ash Grove Agg./Butler, MO	Yes
Iron Mt. Trap Rock (Felsite)	Pilot Knob	Iron Mt. Trap Rock Co./Iron Mt., MO	Yes
Jefferson City Dolomite	Jefferson City-Cotter	Capital Quarries/Rolla, MO	Yes
Little Piney River Gravel	Quaternary Alluvium	Capital Quarries/Rolla, MO	No
Meramec River Gravel	Quaternary Alluvium	Winter Bros. Quarries/St. Louis, MO	No
Missouri River Gravel	Quaternary Alluvium	Capital Quarries/Jefferson City, MO	No
Osage River Gravel	Quaternary Alluvium	Capital Quarries/Jefferson City, MO	No

4.1.2. Control Samples. For the purpose of testing WipShape algorithms, simple control samples that exhibit relatively uniform characteristics were assembled. Samples

of Jefferson City dolomite and Missouri River gravel were individually placed into a mechanical sieve shaker to separate the aggregate into sieve sizes of #4 (passing 3/8" sieve, retained on #4 sieve) and 3/8" (passing 1/2" sieve, retained on 3/8" sieve). All samples were then washed and oven dried, removing unwanted dust from the mechanical shaker. The dolomite provided a crushed (angular) aggregate, while the river gravel provided an uncrushed (rounded) aggregate. For each of the #4 and 3/8" sieve sizes, a mixture of 50 percent dolomite and 50 percent river gravel, by weight, was assembled. The #4 and 3/8" river gravel, dolomite, and 50/50 mixture are presented in Figure 4.1. The scale is in inches.

Control aggregate samples used for the physical tests (except Percentage of Fractured Particles) weighed approximately 6,000 grams, and were reduced to approximately 1,500 grams for testing with the WipShape imaging system. For the purpose of time constraints, the samples processed through the WipShape imaging system were reduced using a mechanical sample splitter in accordance with ASTM C 702. Each control sample was processed through WipShape three times to obtain Minimum Average Curve Radius measurements.

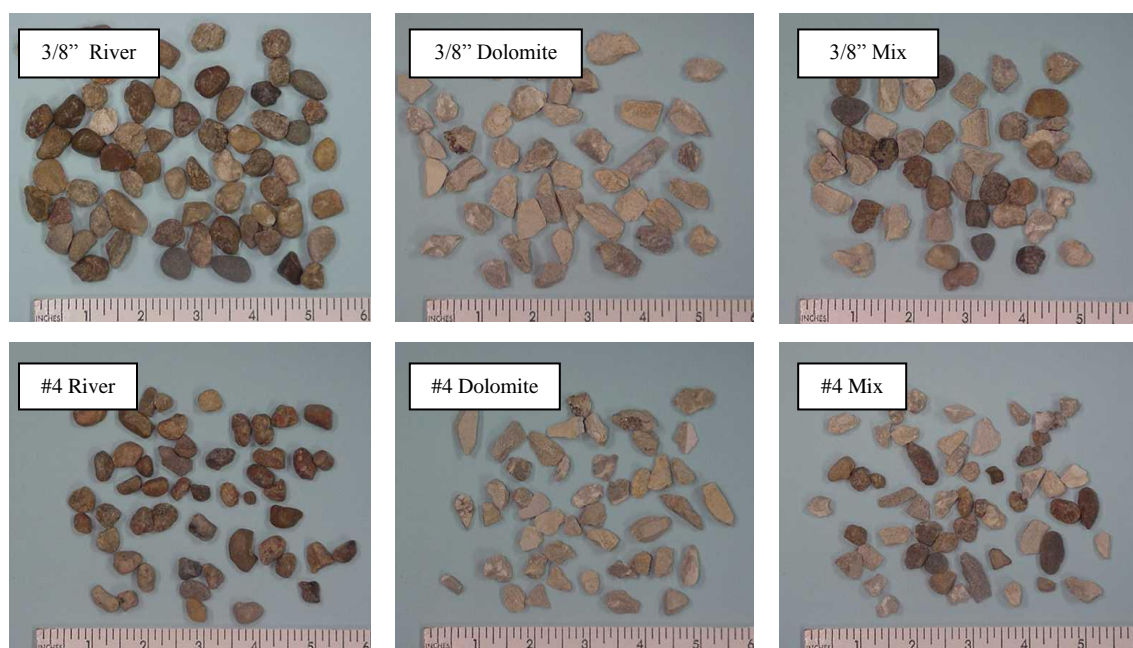


Figure 4.1. Control Samples

4.1.3. Bulk Samples. Seven different bulk samples were individually placed into a mechanical sieve shaker to separate the aggregate into sizes retained on #4, 3/8", 1/2", and 3/4" sieves for physical and WipShape testing. All samples were then washed and oven dried, removing unwanted dust from the mechanical shaker. Table 4.2 provides the individual bulk sample types and sieve sizes used for testing.

Table 4.2. Bulk Samples Used for Testing

Bulk Samples	Sieve Size (Retained)			
	#4	3/8"	1/2"	3/4"
Canadian Limestone	X	X	X	
Higginsville Limestone		X	X	
Iron Mt. Trap Rock	X			
Little Piney River Gravel	X	X	X	X
Meramec River Gravel		X	X	X
Missouri River Gravel			X	
Osage River Gravel	X			

Bulk aggregate samples used for the physical tests (except Percent of Fractured Particles) weighed approximately 6,000 grams, and were reduced to approximately 1,500 grams for testing with the WipShape imaging system. For the purpose of time constraints, the samples processed through the WipShape imaging system were reduced using a mechanical sample splitter in accordance with ASTM C 702. Percent of Fractured Particle test sample sizes ranged from approximately 250 to 600 grams. Pictures of the seven different bulk samples are presented in Appendix A. Each bulk sample was processed through WipShape four times to obtain Minimum Average Curve Radius measurements.

4.2. PHYSICAL LABORATORY TEST METHODS USED

Physical laboratory tests procedures used in this research have been well established and are specified by the American Society of Testing Materials (ASTM) standards and/or American Association of State Highway and Transportation Officials

(AASHTO) standards. The methods are accepted and have been used for years by industry.

4.2.1. Uncompacted Void Content of Coarse Aggregate. This method is AASHTO Designation TP56. The void content of coarse aggregate provides an indication of the aggregates' angularity, sphericity, and surface texture compared with other coarse aggregates tested in the same grading (AASHTO 1999). The test aggregate is allowed to free fall 115mm from the funnel of a cylindrical hopper into a 154mm diameter by 160mm high cylindrical measure. Excess aggregate is struck off, and its mass is determined by weighing. The apparatus used in this method is shown in Figure 4.2.

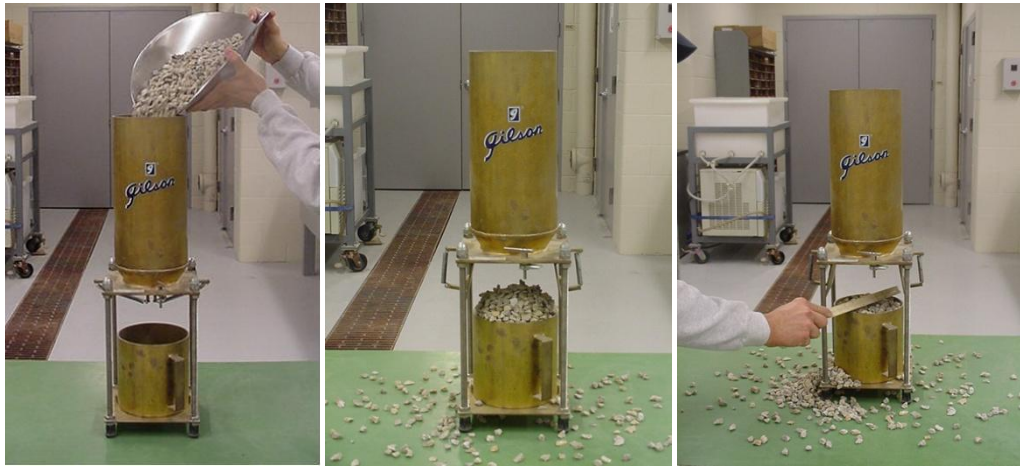


Figure 4.2. Uncompacted Void Content of Coarse Aggregate Apparatus

Uncompacted void content is calculated as the difference between the volume of the cylindrical measure and the absolute volume of the coarse aggregate collected in the measure as shown in equation 2. The bulk dry specific gravity of the coarse aggregate, determined by AASHTO T85 (with review of ASTM C 127), was used in calculating the void content.

$$U = (V - M/S)/V \times 100 \quad (2)$$

An increase in void content of equal-size gradations indicates higher angularity, less rounded (spherical), a rougher surface texture or a combination of these factors. Method B of this test procedure, where individual size fractions are tested separately, was performed for this study. However, results were reported using the individual sizes, a slight modification from Method B, for comparative analysis with WipShape measurements. Control samples were tested for uncompacted void content once, while bulk samples were tested twice.

4.2.2. Index of Aggregate Particle Shape and Texture (Compacted Voids).

This test method provides an index value to the relative particle shape and texture characteristics of aggregates (ASTM D 3398-00). The test aggregate is placed into a 4-inch or 6-inch diameter cylindrical mold, depending on the sieve size fractions, in three equal layers. Aggregates retained on #4 and 3/8" sieves are placed in the 4-inch diameter mold, while aggregates retained on 1/2" and 3/4" sieves are placed in the 6-inch diameter mold. The 6-inch and 4-inch diameter molds with the tamping rods are shown in Figure 4.3.



Figure 4.3. Index of Aggregate Particle Shape and Texture Molds

Each individual layer placed in the molds is compacted by 10 (V10) or 50 (V50) drops with a specified tamping rods. After the final layer has been compacted, individual pieces of aggregate are added to make the surface of the aggregate mass even with the rim of the mold, with no projections above the rim. Mass of the aggregate is determined

and the test is repeated using the same specimen and compaction effort. The average mass of the two tests are used for calculating the percentage of voids. The percentage of voids in each size fraction of the aggregate at 10 drops per layer and 50 drops per layer are determined by the equations 3 and 4.

$$V_{10} = [1 - (M_{10}/SV)] \times 100 \quad (3)$$

$$V_{50} = [1 - (M_{50}/SV)] \times 100 \quad (4)$$

A particle index for each size fraction is determined. Then the weighted particle index of an aggregate containing several sizes is calculated by averaging the particle index data for each size fraction, weighted on the basis of the average grading of the material proposed to be used in the work. In this study, the results are reported using only the percentage of compacted voids in each size fraction for purposes of comparative analysis with WipShape, a slight modification from reporting particle index. The term Compacted Voids is used in place of Index of Particle Shape during this study. Control samples were tested for Compacted Voids once, while bulk samples were tested twice.

4.2.3. Fractured Particles in Coarse Aggregate. This test method provides the percentage, by mass or count, of a coarse aggregate sample that consists of fractured particles meeting specified requirements (ASTM D 5821-01). Each particle of a sample is visually examined and placed into two categories: (1) fractured particles with the required number of fractured faces, and (2) particles not meeting the specified criteria. A face is considered a fractured face only if the maximum projected area is at least as large as one quarter of the maximum projected area of the particle and the face has sharp or slightly blunt edges. The mass, or count, percentage of particles meeting fractured face criteria is reported using equation 5.

$$P = [F/(F + N)] \times 100 \quad (5)$$

This method provides information on the angularity of coarse aggregate. A higher percentage of particles with fractured faces are associated with higher angularity. The sample size was chosen such that the mass of aggregate retained on the 3/4" sieve

exceeded 1500 grams, mass of aggregate retained on the 1/2" sieve exceed 500 grams, and mass of aggregate retained on the 3/8" and #4 sieves exceeded 200 grams.

4.2.4. Bulk Specific Gravity of Coarse Aggregate. This test method provides the relative density (specific gravity) of a quantity of coarse aggregate (AASHTO T85, ASTM C 127-01). Bulk specific gravity was determined for all of the aggregates used in this research for the purpose of determining uncompacted void content and index of particle shape results. Aggregate samples are washed, reduced and immersed in water for 15 to 19 hours. Samples are removed from the water, and rolled in a large absorbent towel until all visible films of water are removed. Mass of the sample is recorded in the saturated-surface-dry condition. Sample is immediately placed in water at $23 \pm 1.7^\circ \text{C}$, to determine its mass. Finally, the sample dried in an oven and mass is determined again. The bulk specific gravity, oven dry, is calculated using equation 6.

$$G_{sb,od} = [A/(B-C)] \times 100 \quad (6)$$

5. COMPARATIVE ANALYSIS OF PHYSICAL AND WIPSHAPE TESTING

5.1. PURPOSE OF COMPARATIVE ANALYSIS

This study was designed to compare and analyze coarse aggregate angularity using well-established physical testing methods and image-based processing. The available, and accepted, measurements of coarse aggregate shape and angularity are few, mostly indirect, time-consuming and tedious. By replacing these labor-intensive physical laboratory tests with image processing techniques, such as the WipShape imaging system, it is believed that characterization of coarse aggregate angularity will become more efficient and productive. The goal of this study is to establish correlations between void content/fractured particles, which are parameters of physical testing, and Minimum Average Curve Radius, which is a parameter of the WipShape imaging system.

5.2. CONTROL SAMPLE TESTING RESULTS

A reasonable correlation between control sample physical test results and WipShape output results would indicate that void content and Minimum Average Curve Radius are correlated.

5.2.1. Uncompacted Void Content and Curve Radius. Figure 5.1 shows a comparative analysis between Uncompacted Void Content and Curve Radius results. The tests were performed on #4 and 3/8" Missouri river aggregate, Jefferson City dolomite aggregate and 50/50 mixture (by weight) of the two.

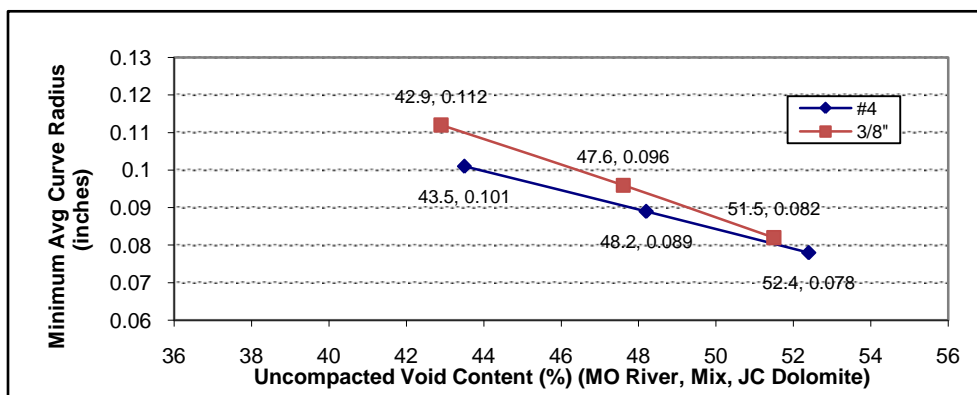


Figure 5.1. Uncompacted Void Content vs. Curve Radius for #4 and 3/8" Control Samples

5.2.2. Compacted Voids and Curve Radius. Figure 5.2 and Figure 5.3 show a comparative analysis between Compacted Voids (V10 and V50) and Curve Radius results. The tests were performed on #4 and 3/8" Missouri river aggregate, Jefferson City dolomite aggregate and 50/50 mixture (by weight) of the two.

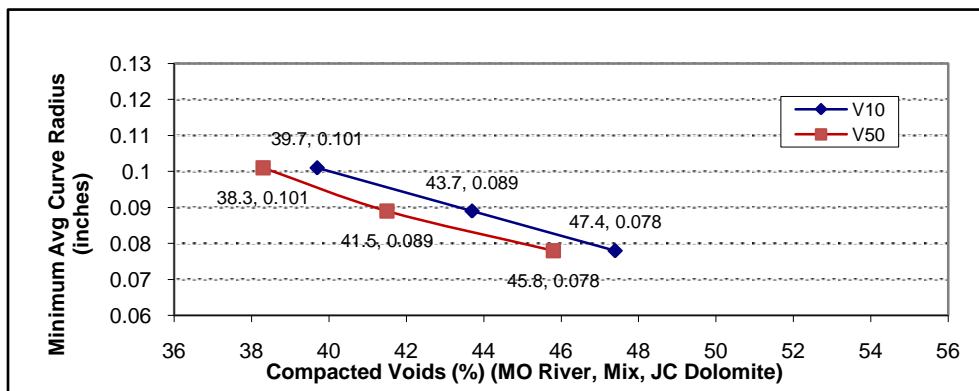


Figure 5.2. Compacted Voids vs. Curve Radius for #4 Control Samples

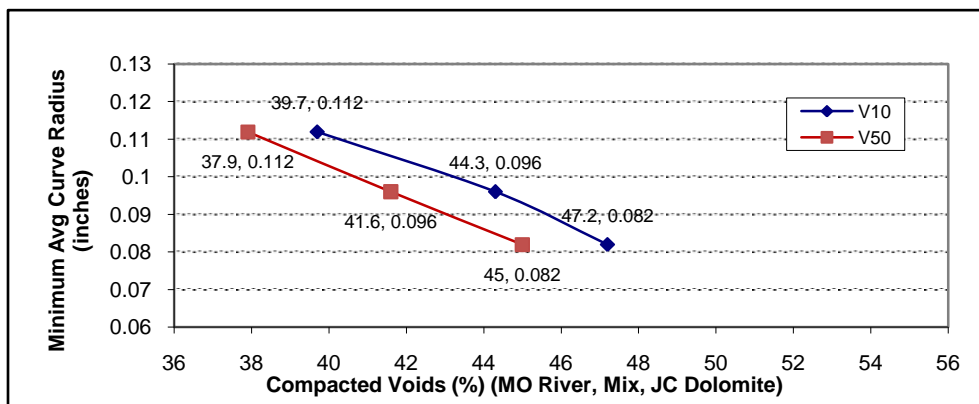


Figure 5.3. Compacted Voids vs. Curve Radius for 3/8" Control Samples

5.2.3. Percentage of Fractured Particles and Curve Radius. Figure 5.4 and Figure 5.5 show a comparative analysis between Percentage of Fractured Particles (Fractured Face Count) and Curve Radius results. The tests were performed on #4 and 3/8" Missouri river aggregate, Jefferson City dolomite aggregate and 50/50 mixture (by weight) of the two.

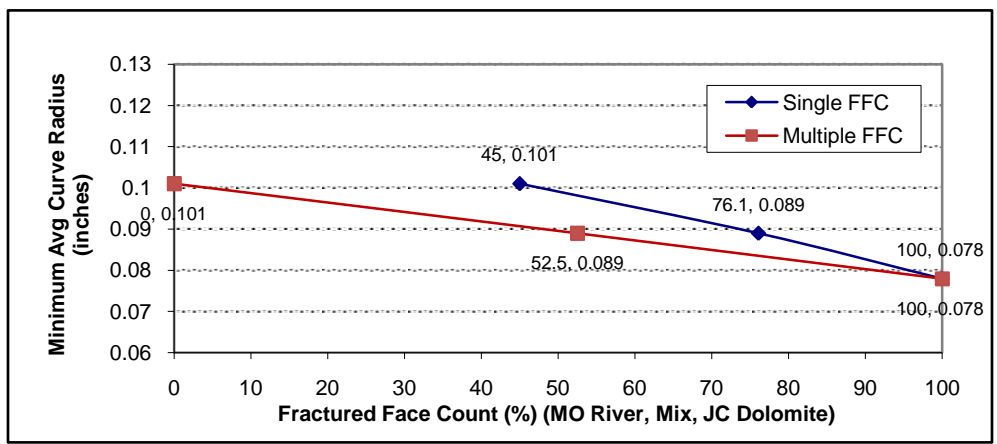


Figure 5.4. Fractured Face Count vs. Curve Radius for #4 Control Samples

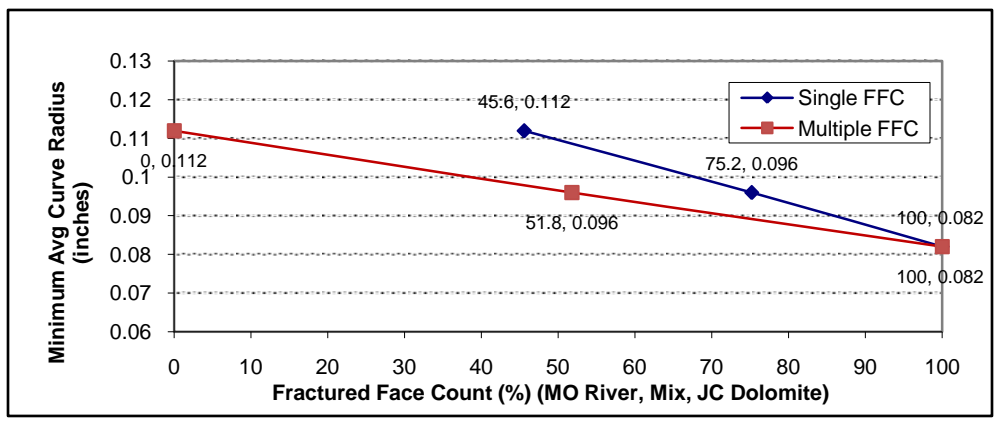


Figure 5.5. Fractured Face Count vs. Curve Radius for 3/8" Control Samples

5.3. ANALYSIS OF CONTROL SAMPLE RESULTS

The results of the control sample testing data indicate that WipShape measurements of Minimum Average Curve Radius appear to be a good predictor of Uncompacted Void Content, Compacted Voids, and Percentage of Fractured Particles. The linear relationships shown in Figures 5.1, 5.2 and 5.3 between Uncompacted Void Content, Compacted Voids and Curve Radius provide confidence that even though physical test methods and the WipShape imaging system produce results in different units (percent voids vs. inches), a good correlation exists.

In addition to the analysis performed between void content and Curve Radius measurements, results from each of the physical test methods were evaluated.

Comparative analysis results between Uncompacted Void Content and Compacted Voids correlate well between each other and also display linear relationships, indicating that both of these physical tests are measuring values that are similar quantitative measures of control sample aggregate shape and angularity characteristics. The graphs comparing each of the physical test methods are presented in Appendix A.

In general, the larger sized aggregate produces lower void percentages and higher Minimum Average Curve Radii, as shown in the Uncompacted Void Content and Compacted Voids graphs. Moreover, void content is significantly reduced with compaction effort, as shown in the Compacted Voids results.

5.4. BULK SAMPLE TESTING RESULTS

Seven different bulk samples retained on #4, 3/8", 1/2" and 3/4" sieves were assembled and subjected to physical and image testing. Individual bulk sample types and sieve sizes used in the analysis are provided in Table 4.2. Reasonable correlations between bulk sample physical test results and WipShape test results would strengthen the indication that void content and Minimum Average Curve Radius are correlated.

5.4.1. Uncompacted Void Content and Curve Radius. Figures 5.6, 5.7 and 5.8 show a comparative analysis between the Uncompacted Void Content and Curve Radius results for bulk samples. The tests were performed on aggregate retained on the #4, 3/8", 1/2" and 3/4" sieves listed in Table 4.2. The 3/4" graph is presented as Figure B.4 in Appendix B.

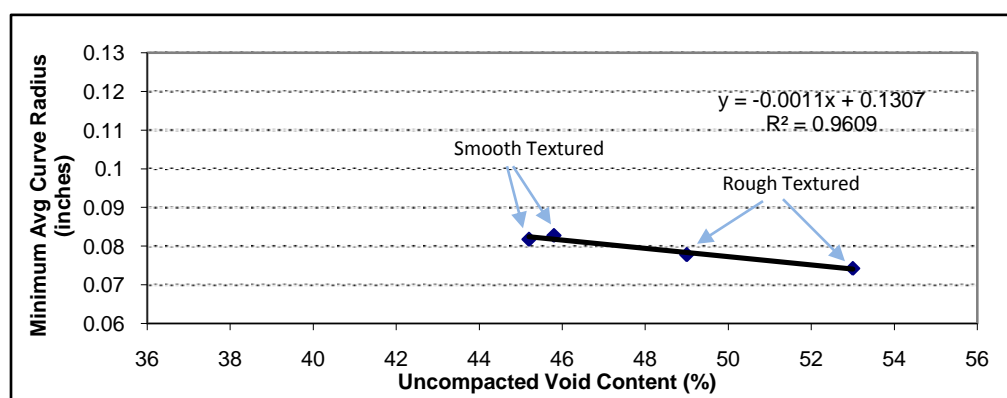


Figure 5.6. Uncompacted Void Content vs. Curve Radius for #4 Bulk Samples

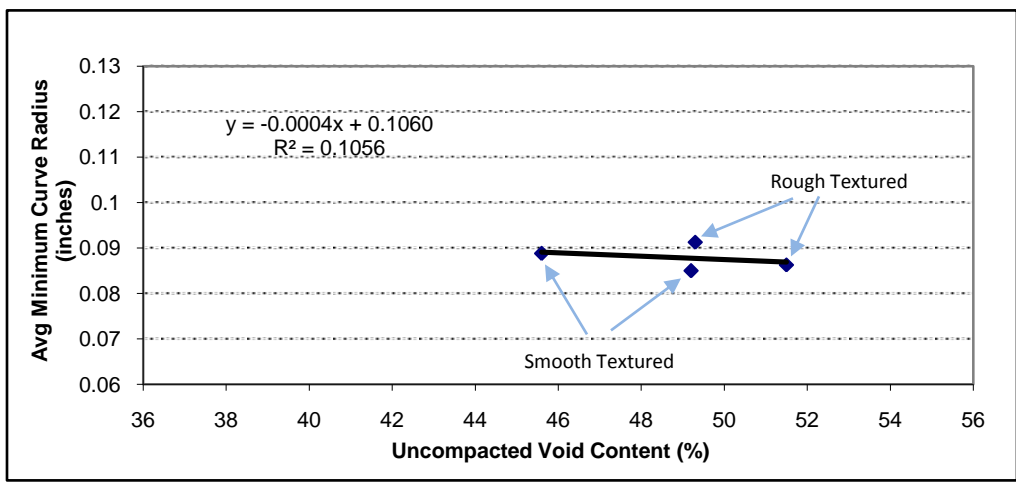


Figure 5.7. Uncompacted Void Content vs. Curve Radius for 3/8" Bulk Samples

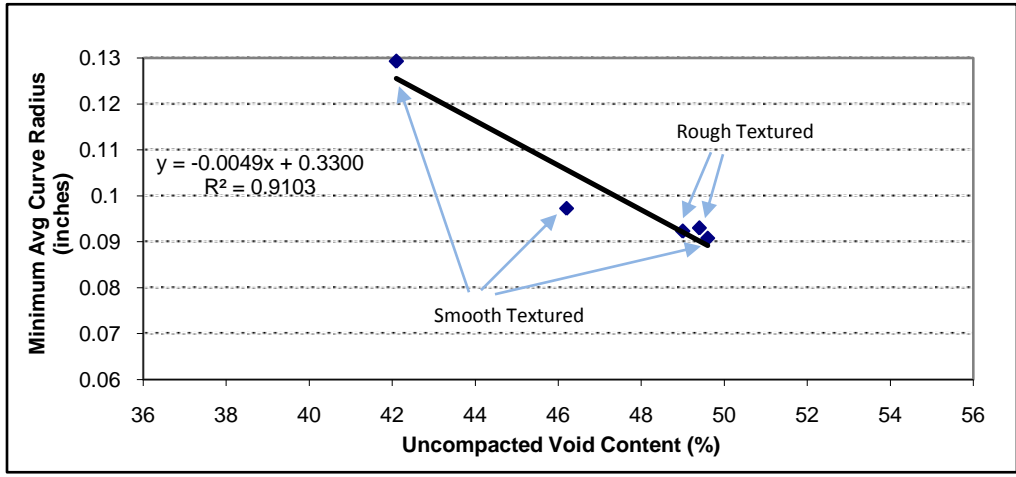


Figure 5.8. Uncompacted Void Content vs. Curve Radius for 1/2" Bulk Samples

5.4.2. Compacted Voids (V10) and Curve Radius. Figures 5.9, 5.10 and 5.11 show a comparative analysis between Compacted Voids, 10 drops per layer, and Curve Radius results for bulk samples. The tests were performed on aggregate retained on the #4, 3/8", 1/2", and 3/4" sieves listed in Table 4.2. The graph for the 3/4" aggregate size is presented as Figure B.8 in Appendix B.

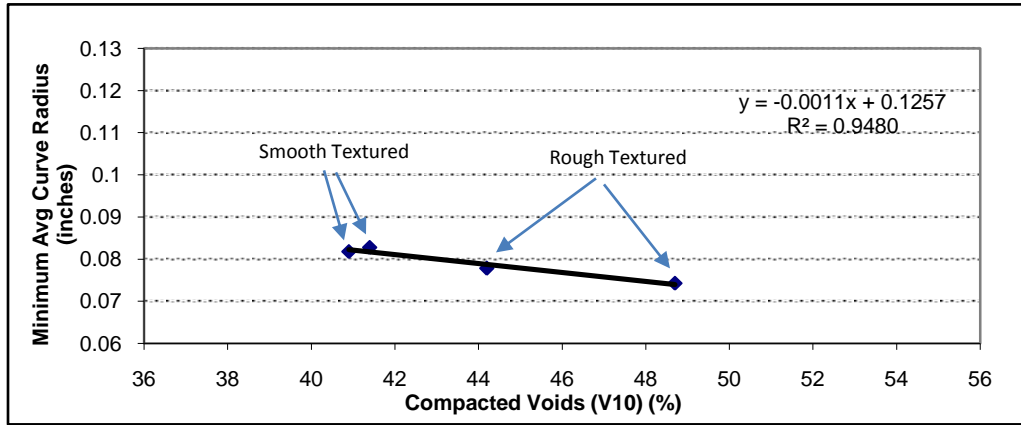


Figure 5.9. Compacted Voids (V10) vs. Curve Radius for #4 Bulk Samples

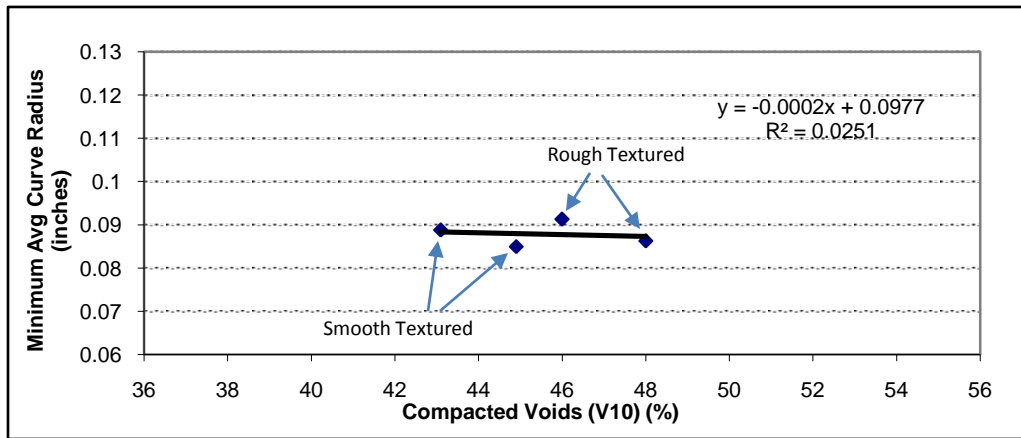


Figure 5.10. Compacted Voids (V10) vs. Curve Radius for 3/8'' Bulk Samples

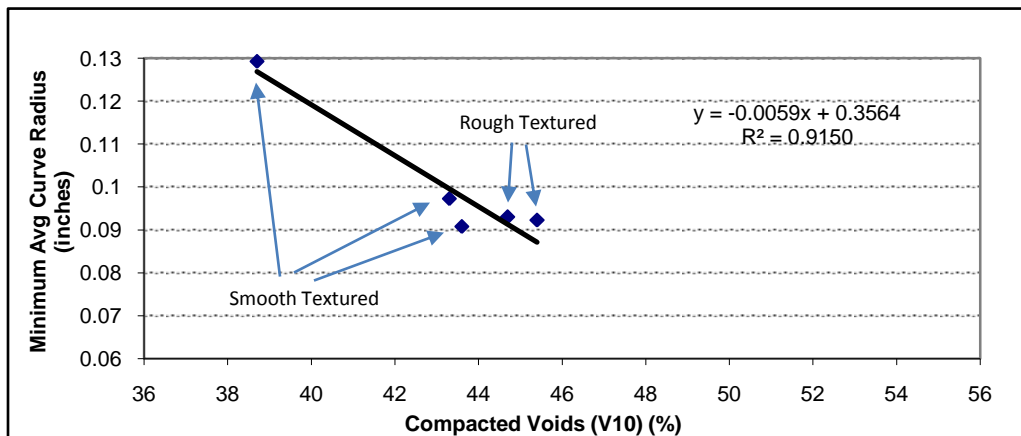


Figure 5.11. Compacted Voids (V10) vs. Curve Radius for 1/2'' Bulk Samples

5.4.3. Compacted Voids (V50) and Curve Radius. Figures 5.12, 5.13 and 5.14 show a comparative analysis between Compacted Voids, 50 drops per layer, and Curve Radius results for bulk samples. The tests were performed on aggregate retained on the #4, 3/8", 1/2", and 3/4" sieves listed in Table 4.2. The graph for the 3/4" aggregate size is presented as Figure B.12 in Appendix B.

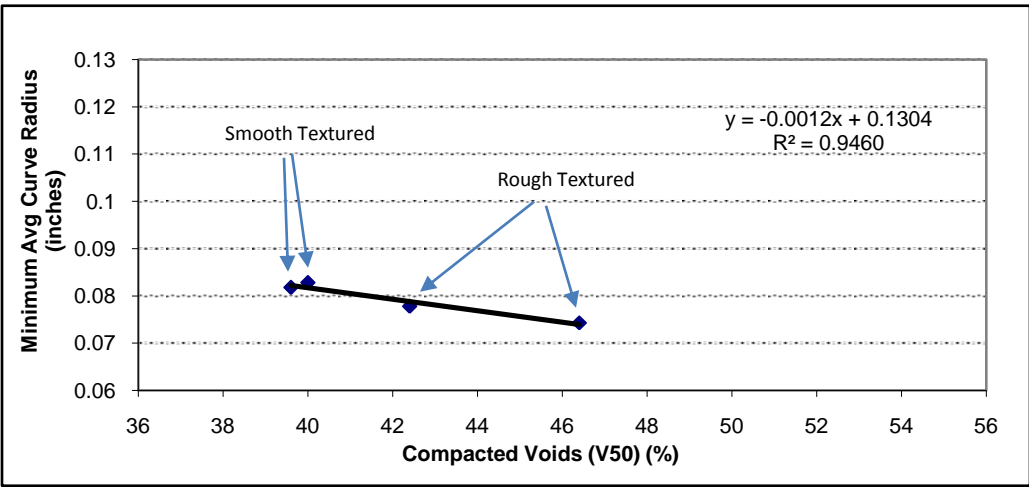


Figure 5.12. Compacted Voids (V50) vs. Curve Radius for #4 Bulk Samples

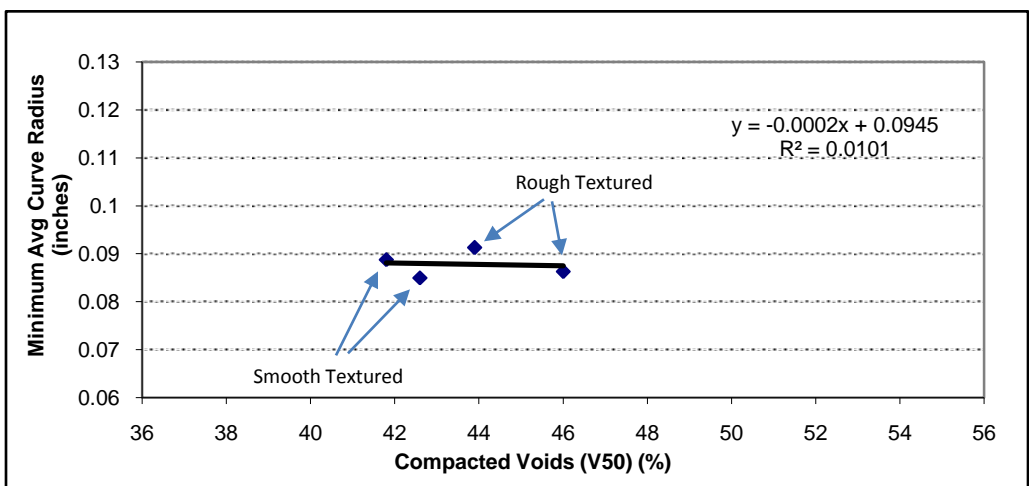


Figure 5.13. Compacted Voids (V50) vs. Curve Radius for 3/8" Bulk Samples

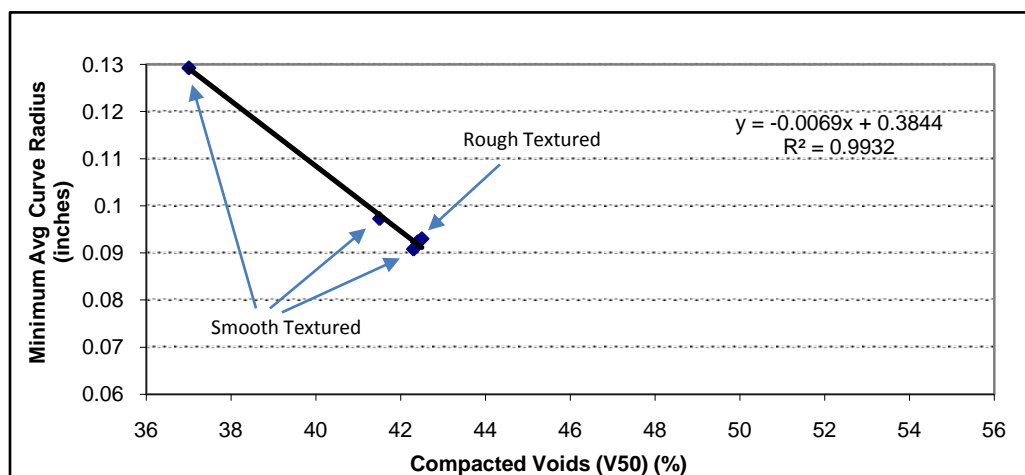


Figure 5.14. Compacted Voids (V50) vs. Curve Radius for 1/2" Bulk Samples

5.4.4. Percentage of Fractured Particles and Curve Radius. A comparative analysis was performed between Percentage of Fractured Particles and Curve Radius results for bulk samples. The tests were performed on aggregate retained on the #4, 3/8", 1/2", and 3/4" sieves listed in Table 4.2. The graphs are presented as Figures B.13, B.14, B.15 and B.18 in Appendix B.

5.5. ANALYSIS OF BULK SAMPLE RESULTS.

Coefficients of determination for bulk aggregate samples retained on the #4 and 1/2" sieves indicate very good linear reliability. The graphs for #4 bulk samples (Figures 5.6, 5.9 and 5.12) show that slopes of the linear regressions are similar for Uncompacted Void Content and Compacted Voids (V10 and V50). However, looking at the 1/2" bulk sample graphs (Figures 5.8, 5.11 and 5.14), the Missouri River samples displayed an unusually high Minimum Average Curve Radius, while the rest of the data was grouped towards the other end of the scale. The increased slope indicates that some non-linearity may be present within the lower void content, but additional samples were not available at this end of the scale to obtain conclusive results. Yet, when closely inspecting the roundness of the 1/2" Missouri River Gravel compared with the other aggregate samples (photographs in Appendix C), the high Curve Radius results are believable. By removing

the rounded Missouri River Gravel sample from the 1/2" Uncompacted Void Content graph, the linear regression slope is decreased significantly as shown in Figure 5.15.

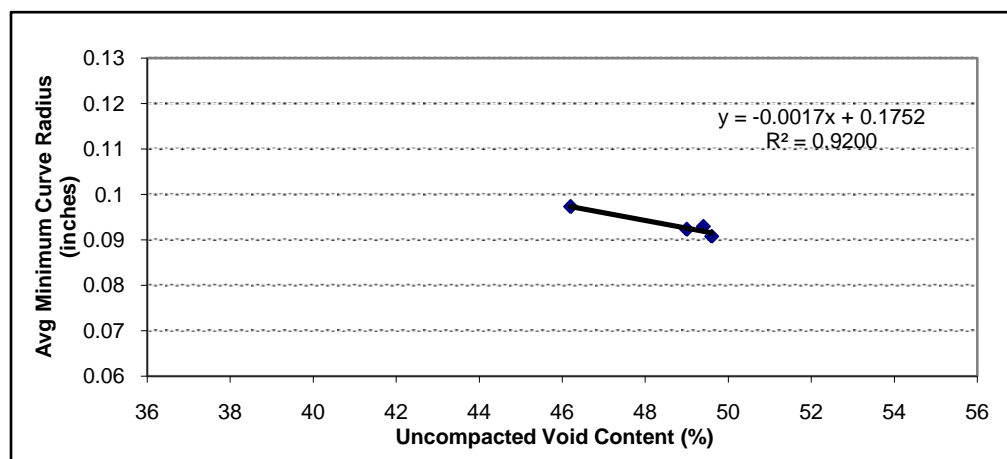


Figure 5.15. Uncompacted Void Content vs. Curve Radius for 1/2" Bulk Samples (without Missouri River Gravel Data)

However, applying the same practice to the Compacted Voids (V10 and V50) graphs, the regression slopes decreased significantly along with the coefficients of determination.

Coefficients of determination for aggregate samples retained on the 3/8" sieve indicate poor linear reliability and the regression slopes are near horizontal, indicating little or no sensitivity to Minimum Average Curve Radius. Looking at the graphs, smaller differences exist between the Minimum Average Curve Radius data points compared to the Uncompacted Void Content and Compacted Voids data points.

Only two samples from the aggregate retained on the 3/4" sieve were tested, so the data does not provide enough information to determine if correlations exist for this size fraction. More samples are needed in this size fraction.

Coefficients of determination for Minimum Average Curve Radius versus Single Fractured Face Counts indicate poor linear reliability, with exception to aggregate retained on the #4 sieve. Regression slopes are near horizontal for the #4, 3/8" and 1/2" aggregate. The results demonstrated the extreme ranges of Percent of Fractured Particles

between the river gravel and crushed stone. The uncrushed river gravel samples typically had very low percentages of single Fractured Face Counts while crushed stone samples had 100 percent of single Fractured Face Counts.

5.6. REPEATABILITY OF BULK SAMPLE TESTING.

Repeatability, or single-operator precision, can be defined as the variation in measurements taken by a single person on the same equipment in the same laboratory within a time span of a few days, and can be calculated by the following equation (Smith and Collins 2001).

$$r = 1.96\sqrt{2} \sigma \quad (7)$$

Sigma (σ) is the single operator standard deviation. The standard deviation is useful as a measure of variation within a given set of data and can be calculated by the following equation.

$$\sigma = \sqrt{\frac{\sum_{i=1}^n (x_i - \bar{x})^2}{n-1}} \quad (8)$$

However, comparing repeatability results that contain different magnitudes and units, the results may be fallacious. Since void content and Minimum Average Curve Radius are presented in different magnitudes and units, repeatability results were normalized by dividing each repeatability result by the mean of the two trials and expressing the normalized repeatability as a percentage. This produces a measure of relative variation rather than absolute variation. The repeatability between results of two trials for each of the Uncompacted Void Content, Compacted Voids (V10 and V50) and Minimum Average Curve Radius are presented in Table 5.1.

Table 5.1. Repeatability for Bulk Sample Testing

Sample	Uncompacted Void Content			Compacted Voids (V10/V50)			Min. Avg. Curve Radius			
	Trial #1 (%)	Trial #2 (%)	N. R. (%)	Trial #1 (%)	Trial #2 (%)	N. R. (%)	Trial #1 (in.)	Trial #2 (in.)	N. R. (%)	
Retained on #4 Sieve										
Canadian	49.6	48.4	4.800	44.2/42.3	44.1/42.4	0.444/0.463	0.077	0.075	5.158	
Iron Mt.	53.2	52.8	1.479	48.7/46.3	48.6/46.4	0.403/0.423	0.073	0.075	5.297	
Meramec	46.1	45.5	2.568	41.4/40.0	41.3/40.0	0.474/0	0.080	0.084	9.561	
Osage	45.3	45.0	1.302	40.9/39.6	41.0/39.6	0.479/0	0.083	0.083	0	
Average			2.537	Average			0.450/0.221	Average		5.004
Retained on 3/8" Sieve										
Canadian	49.7	48.8	3.582	46.4/44.3	45.6/43.5	3.409/3.572	0.092	0.092	0	
Higginsville	52.1	50.8	4.952	48.5/46.8	47.5/45.1	4.083/7.251	0.090	0.084	13.517	
Little Piney	48.9	49.4	1.994	44.7/42.2	45.1/43.0	1.746/3.681	0.084	0.084	0	
Meramec	46.0	45.2	3.439	43.3/42.0	42.8/41.5	2.276/2.347	0.087	0.087	0	
Average			3.492	Average			2.879/4.213	Average		3.379
Retained on 1/2" Sieve										
Canadian	49.3	48.6	2.803	45.4/42.2	45.3/42.6	0.196/1.849	0.092	0.092	0	
Higginsville	49.8	48.9	3.574	44.6/42.5	44.7/42.5	0.196/0	0.092	0.092	0	
Little Piney	48.5	50.7	8.694	43.6/42.3	43.6/42.3	0/0	0.090	0.089	2.190	
Meramec	45.6	46.8	5.091	43.4/41.4	43.2/41.5	0.392/0.196	0.097	0.096	2.031	
Missouri	42.5	41.6	4.195	38.8/37.1	38.5/36.9	0.588/0.392	0.128	0.129	1.525	
Average			5.388	Average			0.716/0.383	Average		1.437
*N.R.= Normalized Repeatability										
**Lower Repeatability indicates more precise measurements.										

For most cases the repeatability is generally low. Compacted Voids (V10 and V50) repeatability results were lower than Minimum Average Curve Radius and Uncompacted Void Content results for all sample sizes, with exception to the V50 aggregate retained on the 3/8" sieve. Repeatability results for the Minimum Average Curve Radius were the worst for aggregate retained on the #4 sieve, but appeared to improve as the aggregate sizes increased. Conversely, repeatability for the Uncompacted Void Content appeared to worsen as the aggregate sizes increased.

5.7. LIMITATIONS OF THE STUDY

Even though a number of good preliminary correlations were found between Minimum Average Curve Radius and physical tests, there are some limitations to the study. The WipShape imaging system has capabilities to determine coarse aggregate shape and size properties such as flat and elongated ratios, gradations and Minimum Average Curve Radius (a measurement of angularity). However, the system currently does not make an objective measurement of coarse aggregate surface texture, while standard physical test procedures appear to provide an indirect estimation of surface profile roughness or irregularity. Also, the scope of this study was limited to seven bulk samples. Additional samples in all sieve sizes might have produced more conclusive testing results.

6. CONCLUSIONS

6.1. CONCLUSIONS

The results of the control sample testing data indicate that WipShape measurements of Minimum Average Curve Radius appear to be a good predictor of Uncompacted Void Content, Compacted Voids, and Percentage of Fractured Particles. The linear relationships between Uncompacted Void Content, Compacted Voids and Curve Radius provide confidence that even though physical test methods and the WipShape imaging system produce results in different units (percent voids vs. inches), a good correlation exists. In addition to the analysis performed between void content and Curve Radius measurements, results from each of the physical test methods were evaluated. Comparative analysis results between Uncompacted Void Content and Compacted Voids correlate well between each other and also display linear relationships, indicating that both of these physical tests are measuring values that are similar quantitative measures of control sample aggregate shape and angularity characteristics.

Coefficients of determination for bulk aggregate samples retained on the #4 and 1/2" sieves indicate very good linear reliability. The graphs for #4 bulk samples (Figures 5.6, 5.9 and 5.12) show that slopes of the linear regressions are similar for Uncompacted Void Content and Compacted Voids (V10 and V50). However, looking at the 1/2" bulk sample graphs (Figures 5.8, 5.11 and 5.14), the Missouri River samples displayed an unusually high Minimum Average Curve Radius, while the rest of the data was grouped towards the other end of the scale. Yet, when closely inspecting the roundness of the 1/2" Missouri River Gravel compared with the other aggregate samples, the high Curve Radius results are believable. By removing the rounded Missouri River Gravel sample from the 1/2" Uncompacted Void Content graph, the linear regression slope is decreased significantly as shown in Figure 5.15. Hence, non-linearity may exist when a larger, well rounded aggregate sample is introduced. However, additional samples were not available at this end of the scale to obtain conclusive results.

Coefficients of determination for aggregate samples retained on the 3/8" sieve indicate poor linear reliability and the regression slopes are near horizontal, indicating little or no sensitivity to Minimum Average Curve Radius. Looking at the graphs,

smaller differences exist between the Minimum Average Curve Radius data points compared to the Uncompacted Void Content and Compacted Voids data points. The reason for the poor linear reliability and near horizontal regression slope is not certain. However, it is believed that differences in surface texture of the aggregate may be a cause. Surface texture or “roughness” of the aggregates used in this study is difficult to observe from the photographs in Appendix C. However, while handling the river gravel aggregates, they were obviously not as rough as the crushed aggregates. Typically, a rough surface texture will produce higher void percentages than a smooth surface texture when comparing aggregates of the same size and angularity. The Little Piney and Meramec River Gravels used in the 3/8” graphs are smooth, but still somewhat angular. Even though the edges of these two river gravels are slightly rounded, they have similar parameters of shape and angularity as the 3/8” Canadian and Higginsville Limestone aggregates. Provided that the shape and angularity characteristics between the 3/8” river gravel and crushed stone samples are similar, it is possible that the Uncompacted Void Content and Compacted Voids tests were affected by the texture differences, creating a larger spread in void percentage values, while the Minimum Average Curve Radius measurements indicated little or no variation due to the inability to measure texture. It is believed this inability to measure texture may be the reason for the insensitivity of the 3/8” samples to Minimum Average Curve Radius.

Only two samples from the aggregate retained on the 3/4” sieve were tested, so the data does not provide enough information to determine if correlations exist for this size fraction. More samples are needed in this size fraction.

Coefficients of determination for Minimum Average Curve Radius versus Single Fractured Face Counts indicate poor linear reliability, with exception to aggregate retained on the #4 sieve. Regression slopes are near horizontal for the #4, 3/8” and 1/2” aggregate, which are probably a result of the extreme ranges of Percent of Fractured Particles between the river gravel and crushed stone, the insensitivity for 3/8” samples mentioned above, and small differences in Minimum Average Curve Radius measurements produced by WipShape. More samples, possibly consisting of crushed river gravel, are needed to determine if correlations exist between Percent of Fractured Particles and Minimum Average Curve Radius.

Repeatability is generally low for most of the testing methods. Compacted Voids (V10 and V50) repeatability results were lower than Minimum Average Curve Radius and Uncompacted Void Content results for all sample sizes, with exception to the V50 aggregate retained on the 3/8" sieve. Repeatability results for the Minimum Average Curve Radius were the worst for aggregate retained on the #4 sieve, but appeared to improve as the aggregate sizes increased. Conversely, repeatability for the Uncompacted Void Content appeared to worsen as the aggregate sizes increased. The variation in measurements for Uncompacted Void Content would be expected to get worse with increasing grain size due to the process of striking off excess heaped aggregate from the cylindrical measure as shown in Figure 4.2. The larger aggregate particles increased the difficulty of leveling out the top of the cylindrical measure without significantly affecting the mass of the aggregate. Furthermore, trials #1 and #2 on the Uncompacted Void Content were not performed within a span of a few days.

During this study, a number of good correlations were discovered between Uncompacted Void Content, Compacted Voids and Minimum Average Curve Radius. This implies that it may be possible to measure coarse aggregate angularity directly, discontinue the labor-intensive physical tests, and still generate similar results.

6.2. RECOMMENDATIONS FOR FURTHER STUDY

The development of image-based analysis techniques to quantify aggregate shape and angularity properties has provided tools to perform coarse aggregate tests in a time and labor-efficient manner. While good correlations were discovered between physical testing and Minimum Average Curve Radius, poor correlations were also discovered. Additional testing with a larger variety of aggregate samples is suggested to validate the viability of shape and angularity measurements performed by image-based processing.

Current standard physical (manual) testing procedures provide an indirect or overall indication of aggregate surface texture characteristics, but fail to make objective measurements of surface roughness or irregularity. The development of a methodology is needed to identify surface texture attributes and incorporate these attributes, such as a texture coefficient, into aggregate shape and angularity measurements to improve the results of image-based procedures.

APPENDIX A
CONTROL SAMPLE GRAPHS AND TESTING DATA

Figure A.1. Uncompacted Void Content vs. Curve Radius for #4 Aggregate

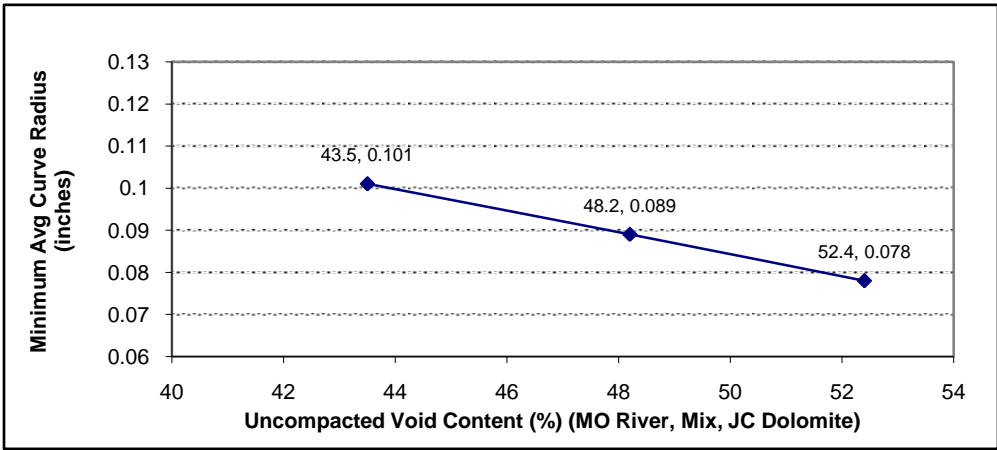


Figure A.2. Uncompacted Void Content vs. Curve Radius for 3/8" Aggregate

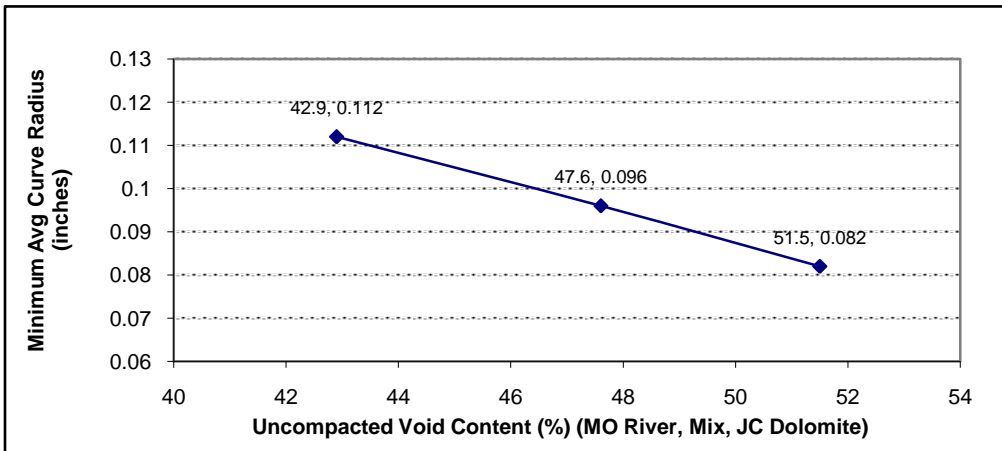


Figure A.3. Compacted Voids vs. Curve Radius for #4 Aggregate

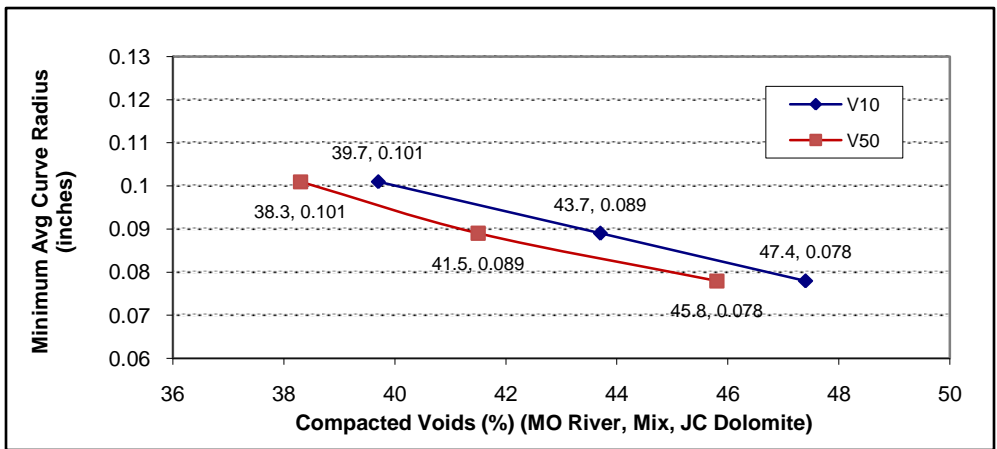


Figure A.4. Compacted Voids vs. Curve Radius for 3/8" Aggregate

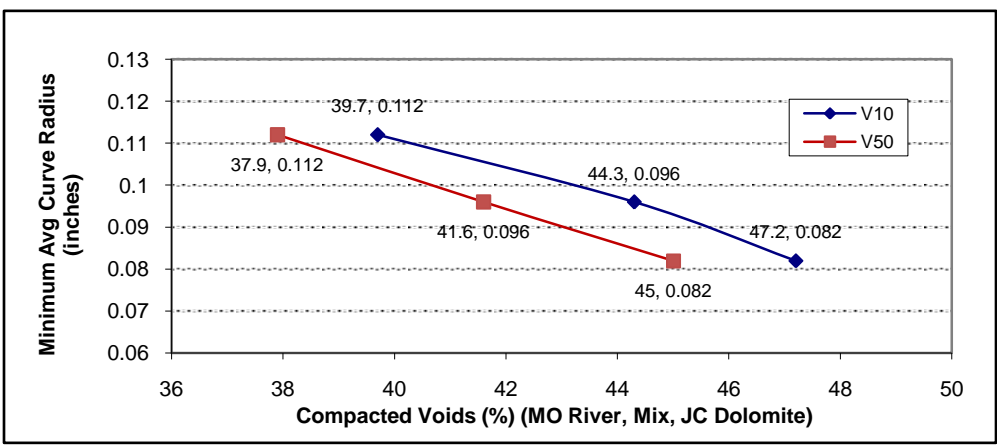


Figure A.5. Fractured Face Count vs. Curve Radius for #4 Aggregate

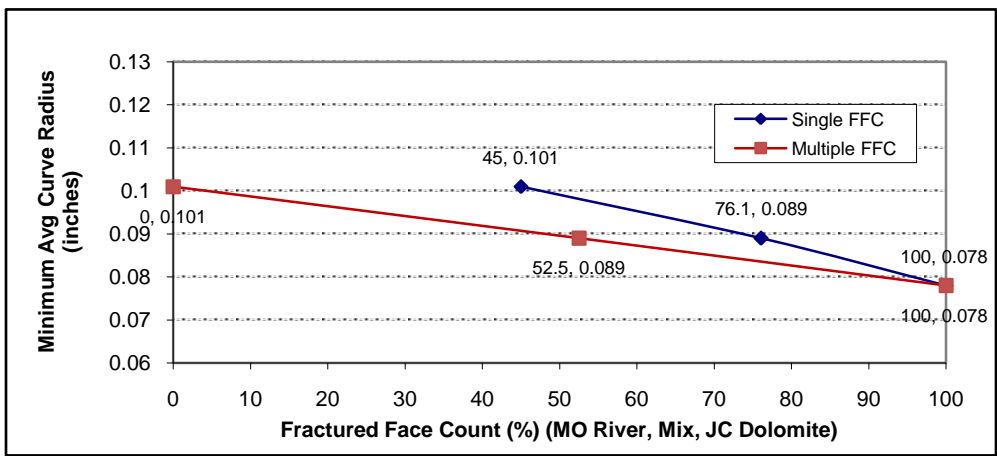


Figure A.6. Fractured Face Count vs. Curve Radius for 3/8" Aggregate

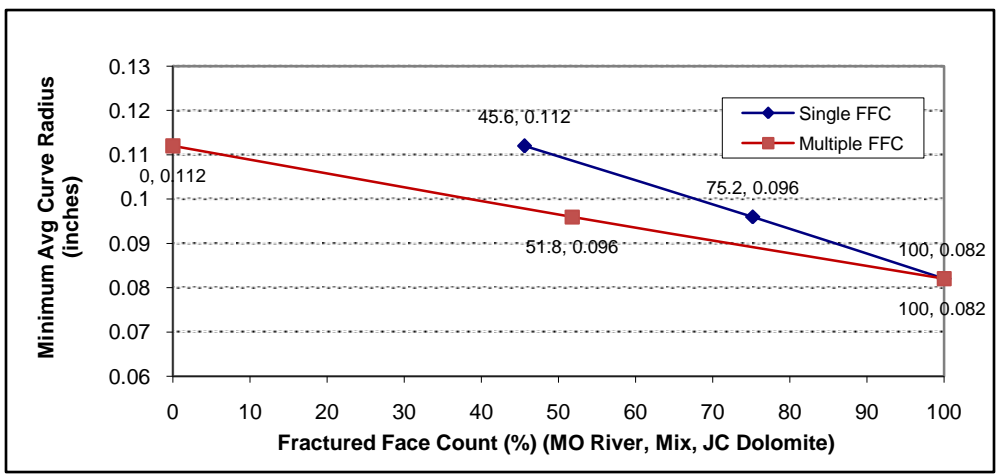


Figure A.7. Uncompacted Void Content vs. Single Fractured Face for #4 Aggregate

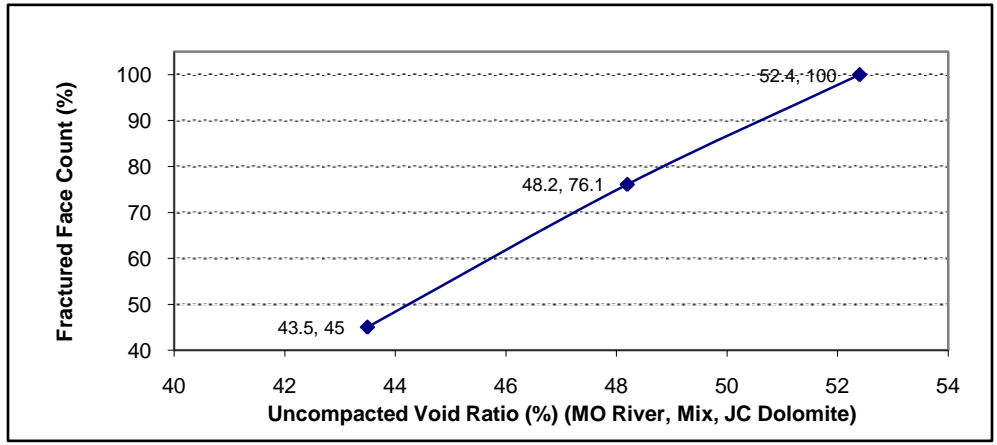


Figure A.8. Uncompacted Void Content vs. Single Fractured Face for 3/8" Aggregate

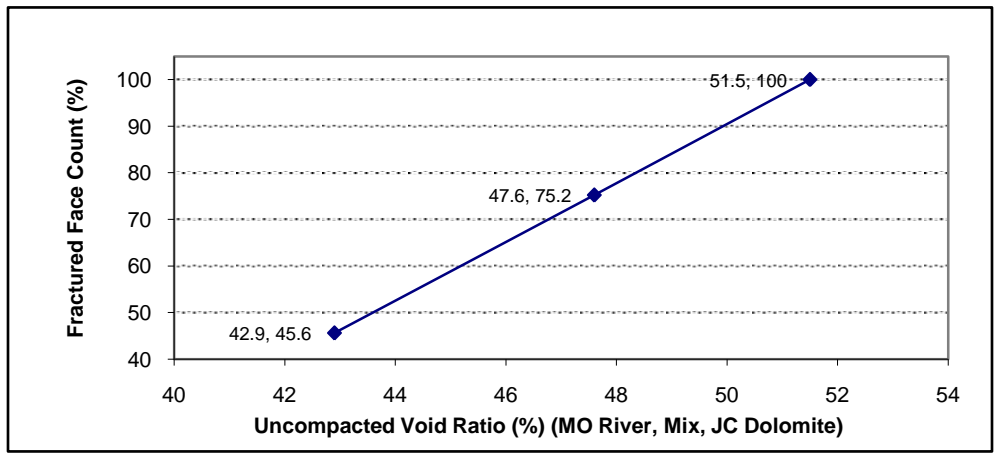


Figure A.9. Uncompacted Void Content vs. Compacted Voids for #4 Aggregate

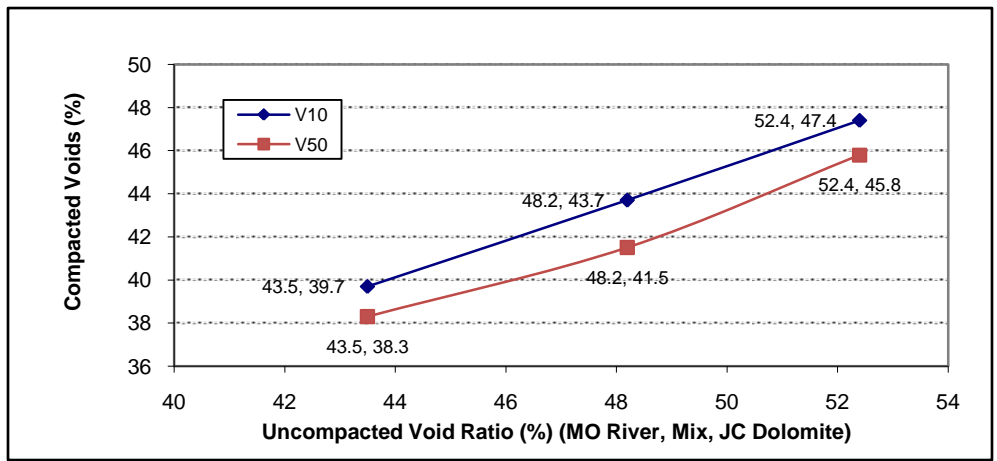


Figure A.10. Uncompacted Void Content vs. Compacted Voids for 3/8" Aggregate

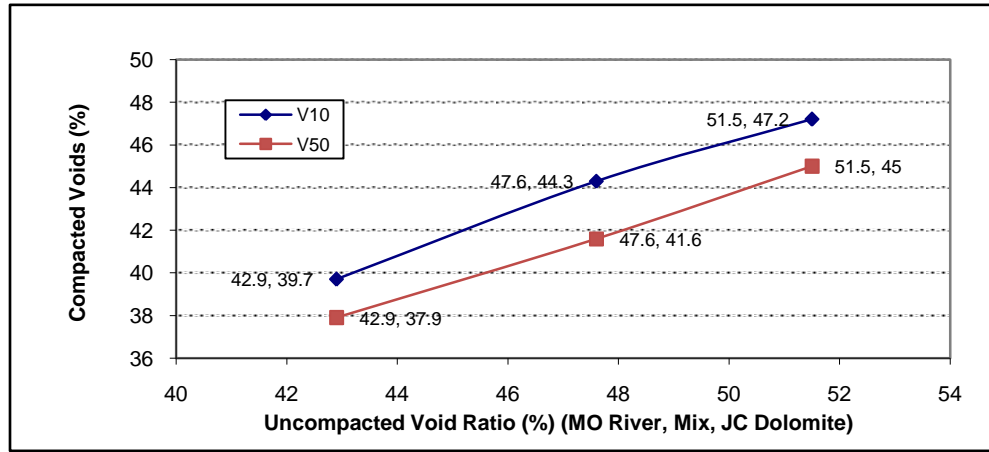


Figure A.11. Single Fractured Face Count vs. Compacted Voids for #4 Aggregate

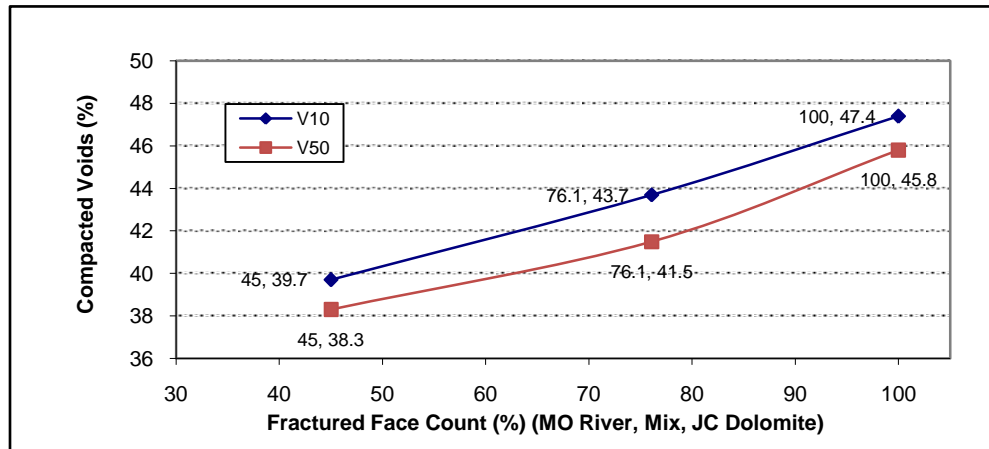


Figure A.12. Single Fractured Face Count vs. Compacted Voids for 3/8" Aggregate

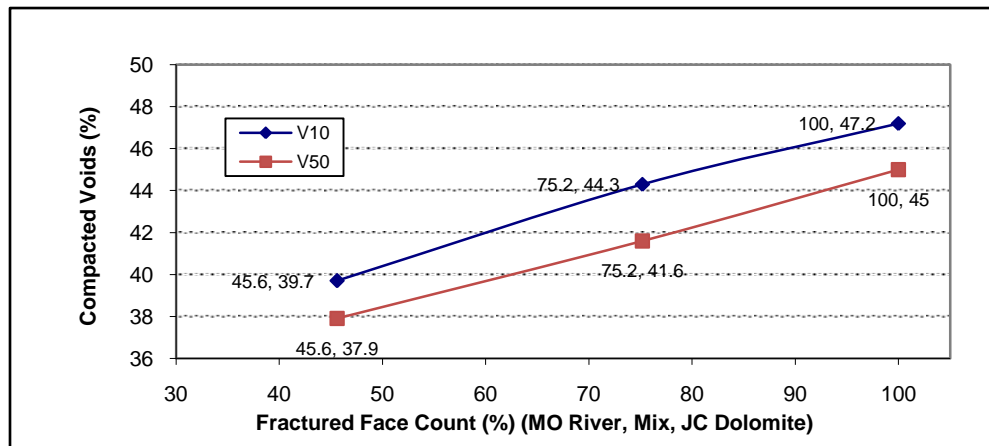


Table A.1. Control Sample Testing Data

Sample	Uncompacted Void Content (%)	Compacted Voids (V10) (%)	Compacted Voids (V50) (%)	Single Fractured Face Count (%)	Multiple Fractured Face Count (%)	Min. Avg. Curve Radius (inches)
Retained on #4 Sieve						
Missouri River	43.5	39.7	38.3	45.0	45.6	0.101
50/50 Mix	48.2	43.7	41.5	76.1	75.2	0.089
Jefferson City	52.4	47.4	45.8	100.0	100.0	0.078
Retained on 3/8" Sieve						
Missouri River	42.9	39.7	37.9	0	0	0.112
50/50 Mix	47.6	44.3	41.6	52.5	51.8	0.096
Jefferson City	51.5	47.2	45.0	100.0	100.0	0.082

APPENDIX B
BULK SAMPLE GRAPHS AND TESTING DATA

Figure B.1. Uncompacted Void Content vs. Curve Radius for #4 Aggregate

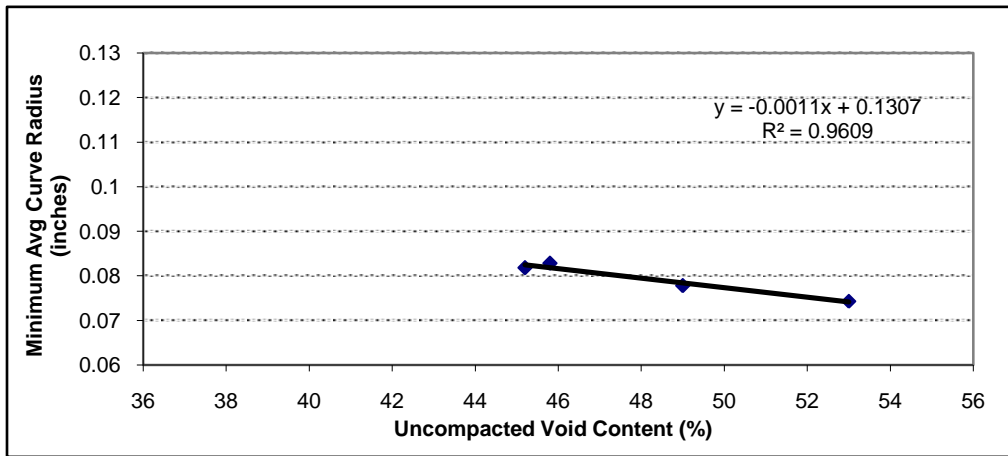


Figure B.2. Uncompacted Void Content vs. Curve Radius for 3/8" Aggregate

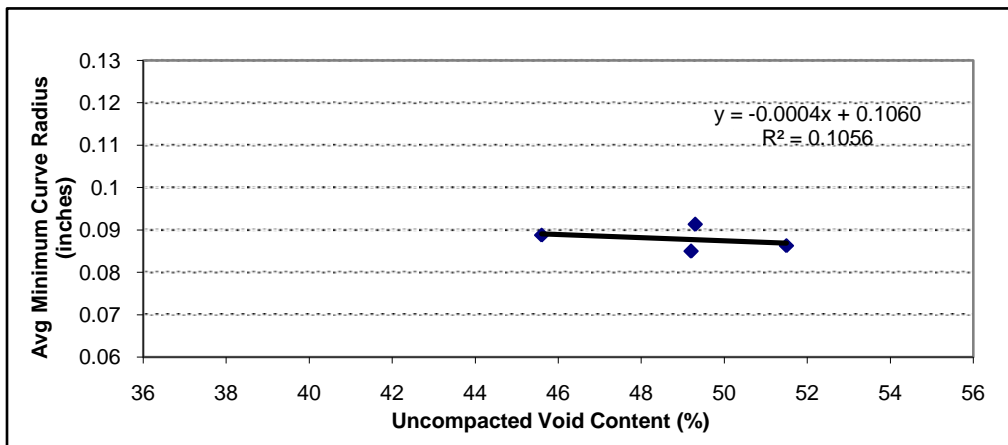


Figure B.3. Uncompacted Void Content vs. Curve Radius for 1/2" Aggregate

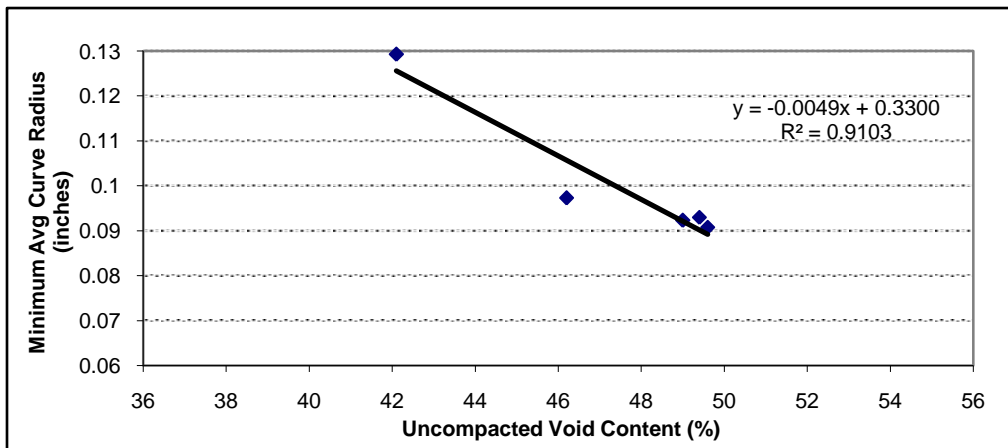


Figure B.4. Uncompacted Void Content vs. Curve Radius for 3/4" Aggregate

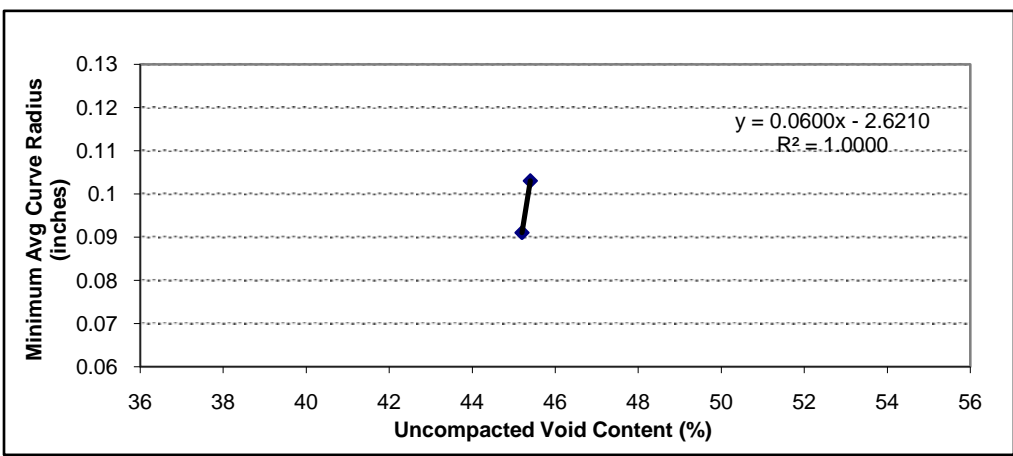


Figure B.5. Compacted Voids (V10) vs. Curve Radius for #4 Aggregate

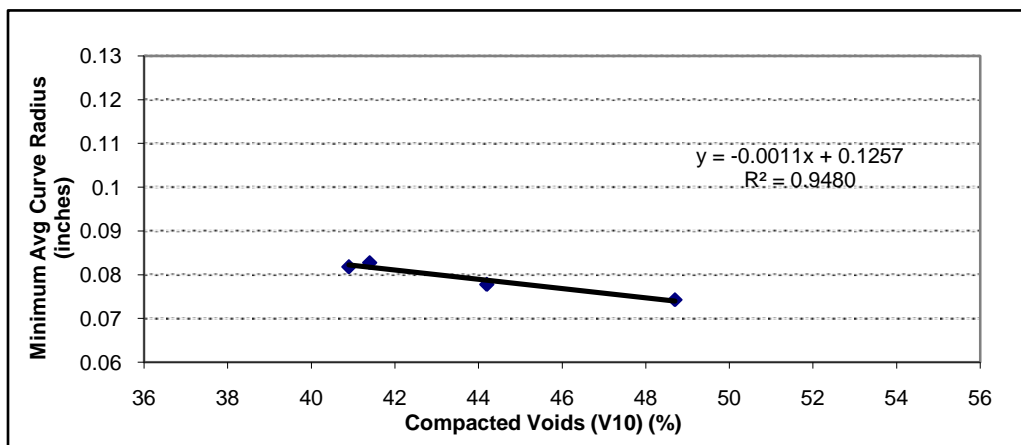


Figure B.6. Compacted Voids (V10) vs. Curve Radius for 3/8" Aggregate

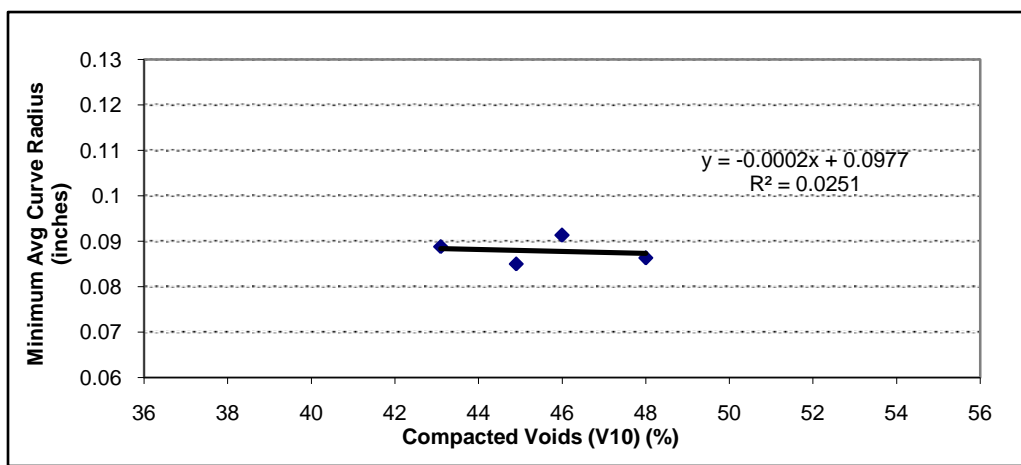


Figure B.7. Compacted Voids (V10) vs. Curve Radius for 1/2" Aggregate

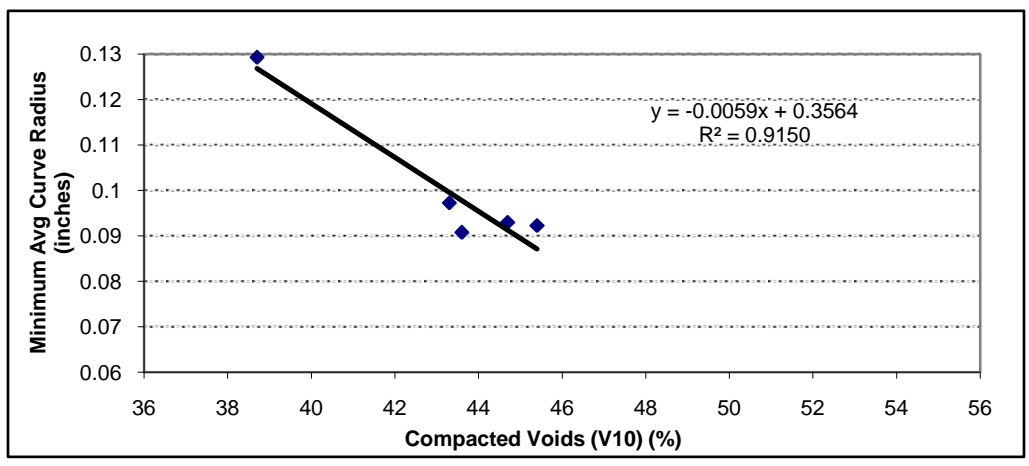


Figure B.8. Compacted Voids (V10) vs. Curve Radius for 3/4" Aggregate

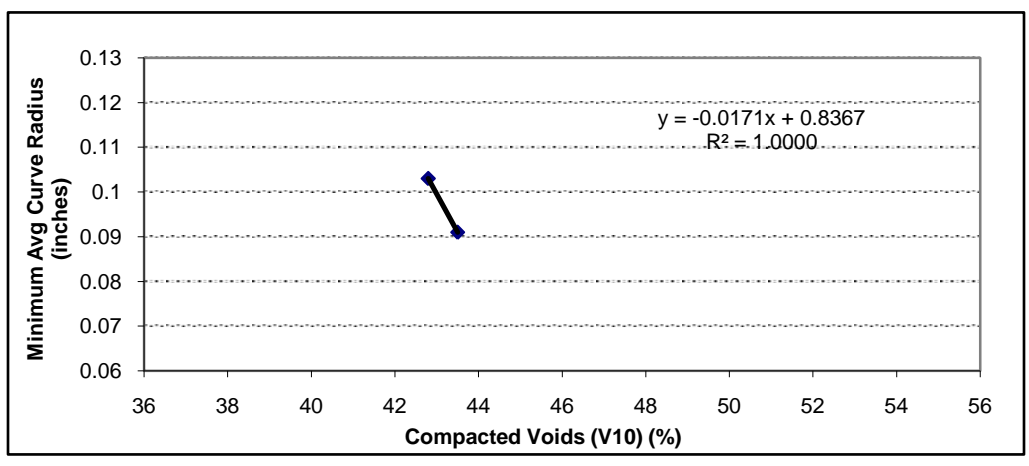


Figure B.9. Compacted Voids (V50) vs. Curve Radius for #4 Aggregate

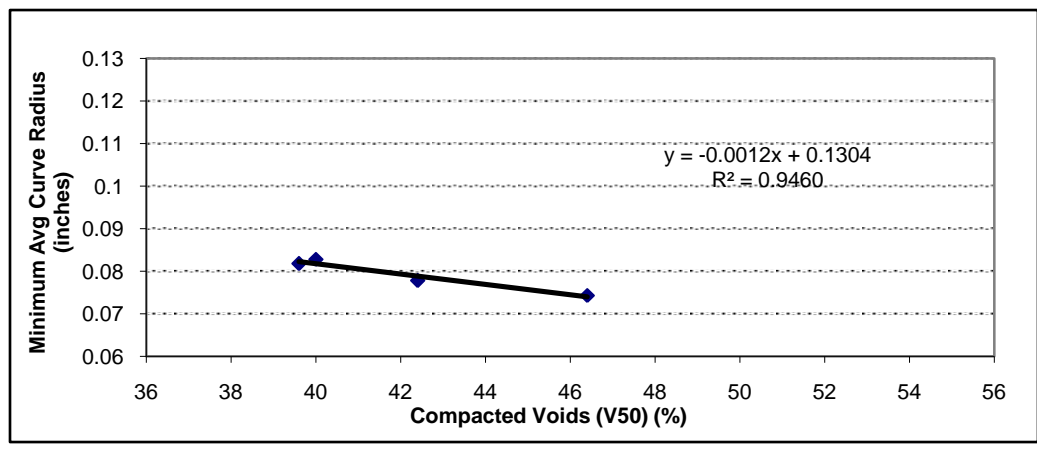


Figure B.10. Compacted Voids (V50) vs. Curve Radius for 3/8" Aggregate

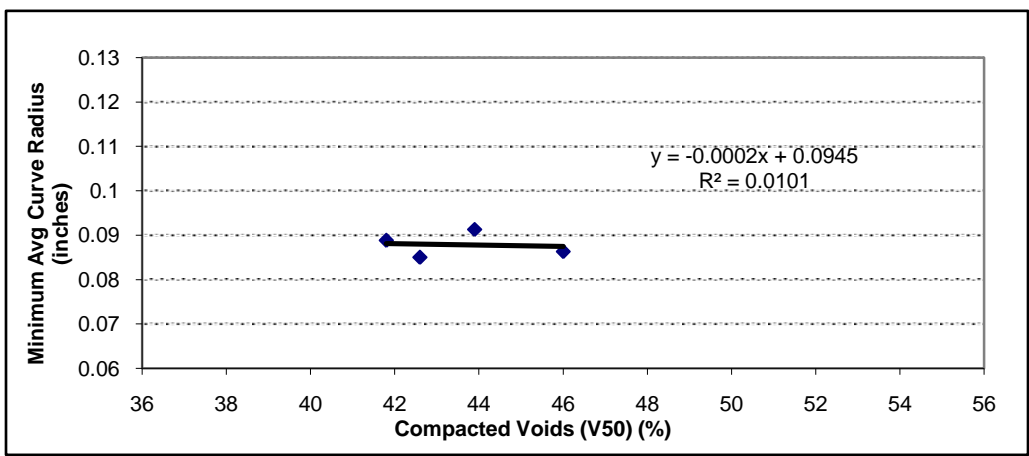


Figure B.11. Compacted Voids (V50) vs. Curve Radius for 1/2" Aggregate

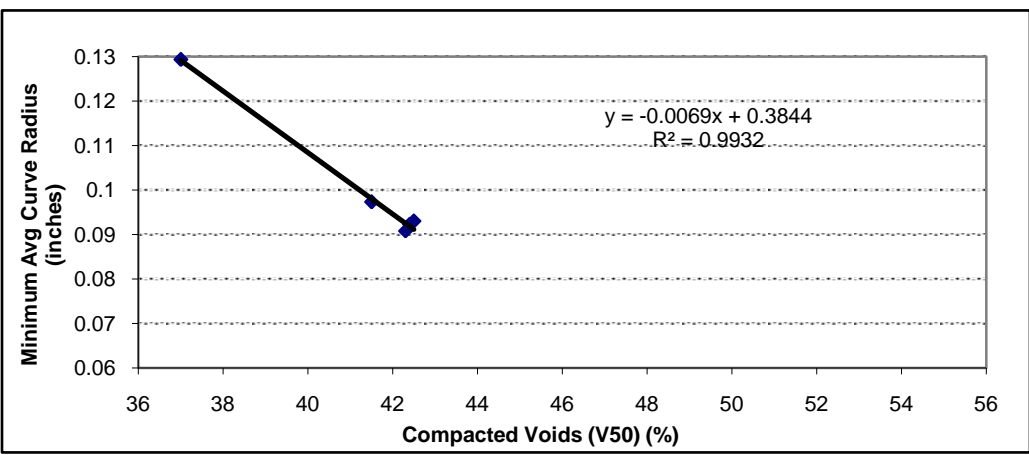


Figure B.12. Compacted Voids (V50) vs. Curve Radius for 3/4" Aggregate

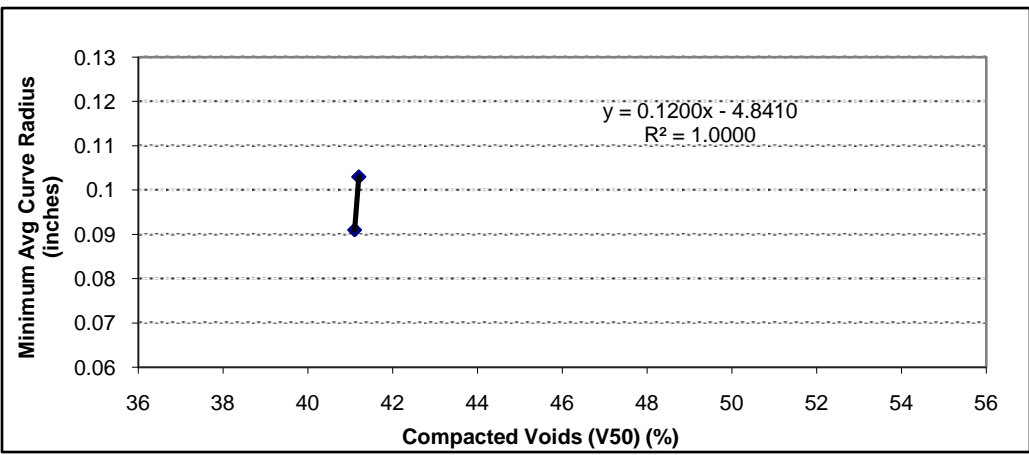


Figure B.13. Single Fractured Face Count vs. Curve Radius for #4 Aggregate

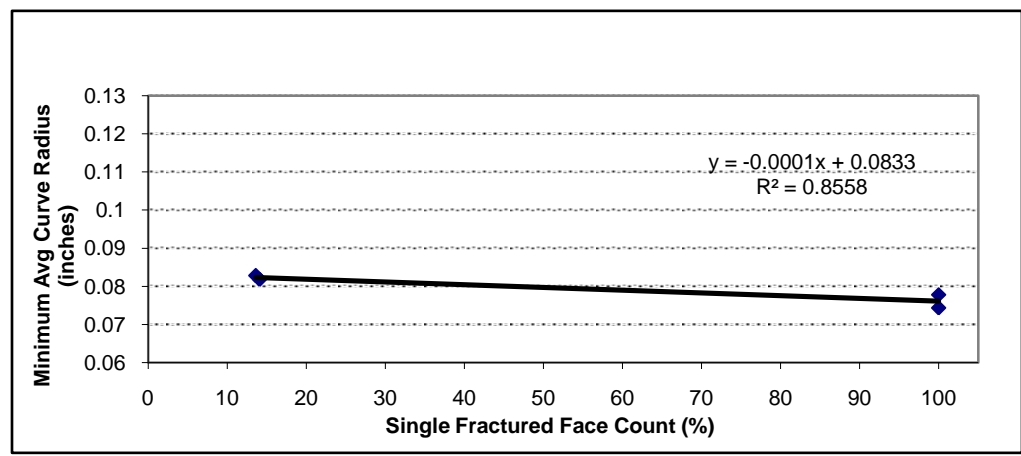


Figure B.14. Single Fractured Face Count vs. Curve Radius for 3/8" Aggregate

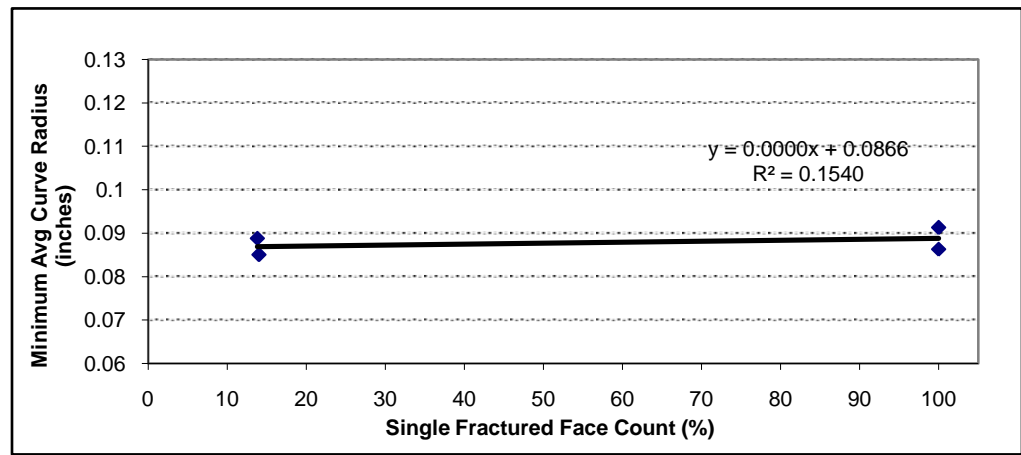


Figure B.15. Single Fractured Face Count vs. Curve Radius for 1/2" Aggregate

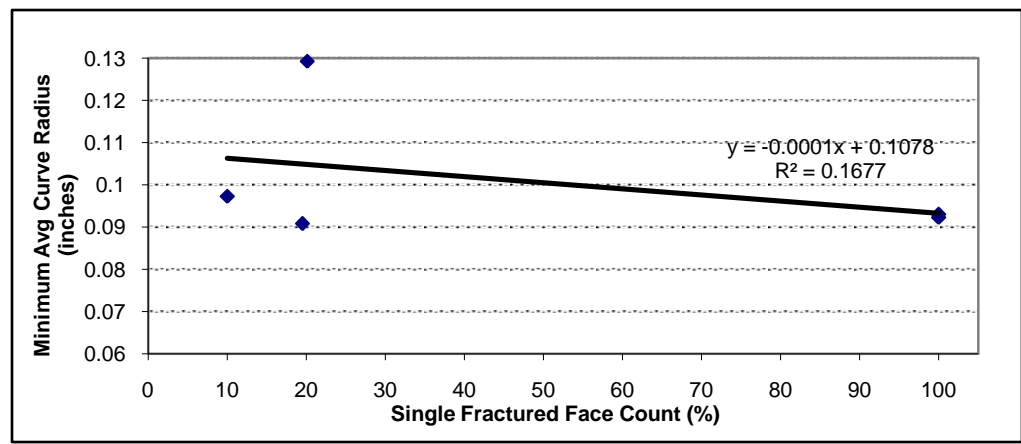


Figure B.16. Single Fractured Face Count vs. Curve Radius for 3/4" Aggregate

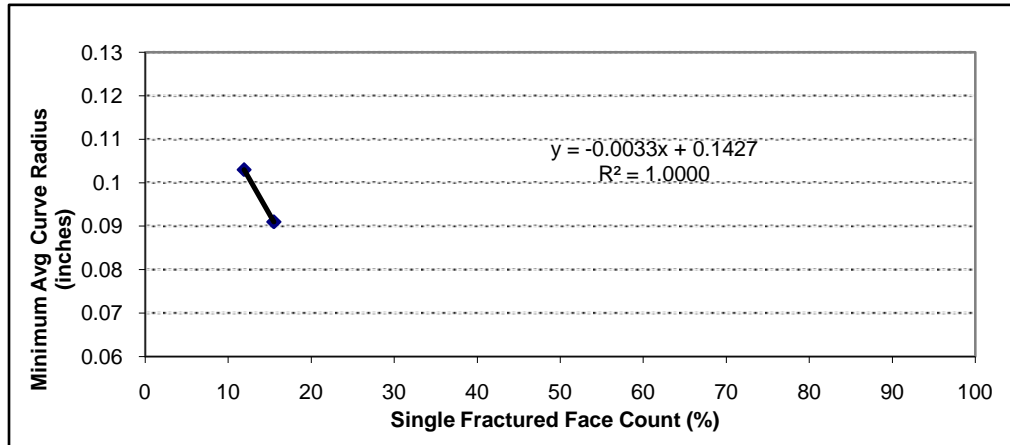


Table B.1. Bulk Sample Testing Data

Sample	Uncompacted Void Content (%)	Compacted Voids (V10) (%)	Compacted Voids (V50) (%)	Single Fractured Face Count (%)	Min. Avg. Curve Radius (inches)
Retained on #4 Sieve					
Canadian Limestone	49.0	44.2	42.4	100.0	0.0778
Iron Mt. Trap Rock	53.0	48.7	46.4	100.0	0.0743
Meramec River	45.8	41.4	40.0	13.6	0.0828
Osage River	45.2	40.9	39.6	14.1	0.0818
Retained on 3/8" Sieve					
Canadian Limestone	49.3	46.0	43.9	100.0	0.0913
Higginsville Limestone	51.5	48.0	46.0	100.0	0.0863
Little Piney River	49.2	44.9	42.6	14.0	0.0850
Meramec River	45.6	43.1	41.8	13.8	0.0888
Retained on 1/2" Sieve					
Canadian Limestone	49.0	45.4	42.4	100.0	0.0923
Higginsville Limestone	49.4	44.7	42.5	100.0	0.0930
Little Piney River	49.6	43.6	42.3	19.5	0.0908
Meramec River	46.2	43.3	41.5	10.0	0.0973
Missouri River	42.1	38.7	37.0	20.1	0.1293
Retained on 3/4" Sieve					
Little Piney River	45.2	43.5	41.1	15.5	0.0910
Meramec River	45.4	42.8	41.2	11.9	0.1030

APPENDIX C
AGGREGATE SAMPLE PHOTOGRAPHS

Figure C.1. Canadian Limestone Aggregate

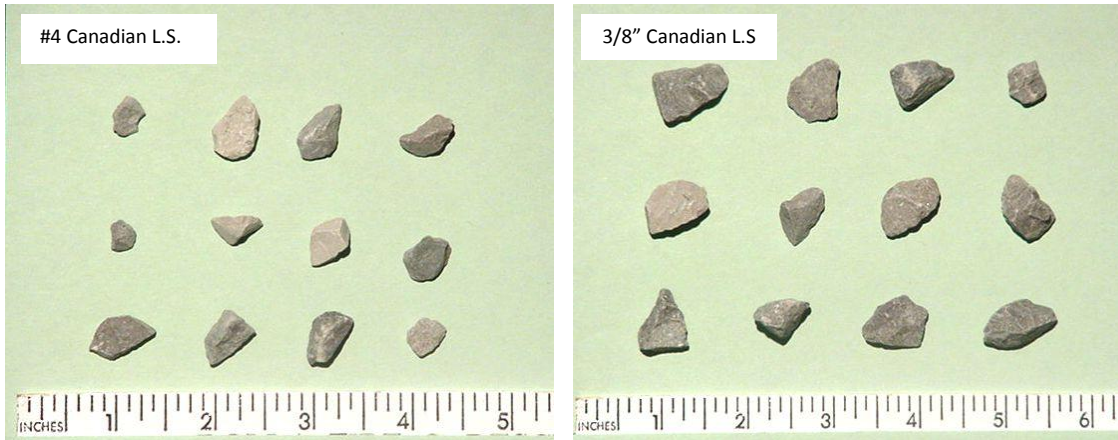


Figure C.2. Canadian Limestone and Higginsville Limestone Aggregate



Figure C.3. Higginsville Limestone and Iron Mt. Trap Rock Aggregate

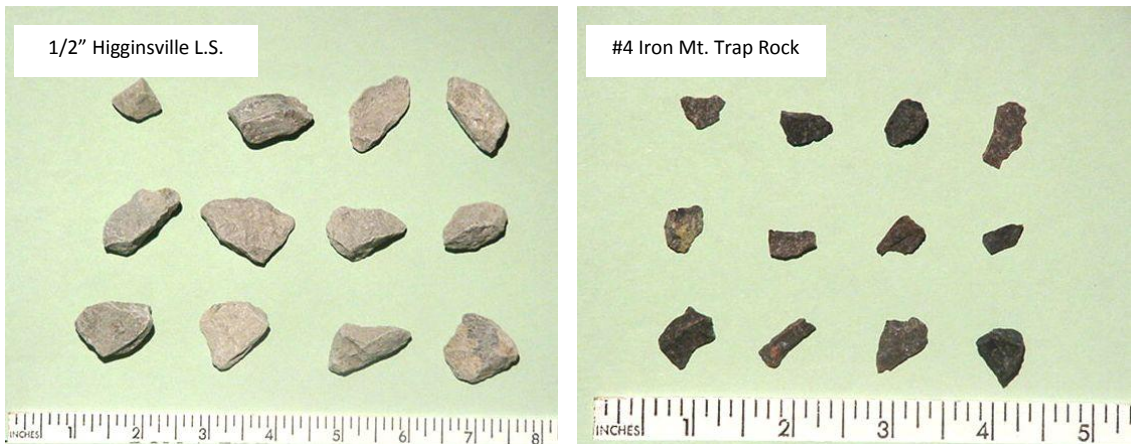


Figure C.4. Jefferson City Dolomite Aggregate



Figure C.5. Little Piney River Aggregate



Figure C.6. Little Piney River and Meramec River Aggregate

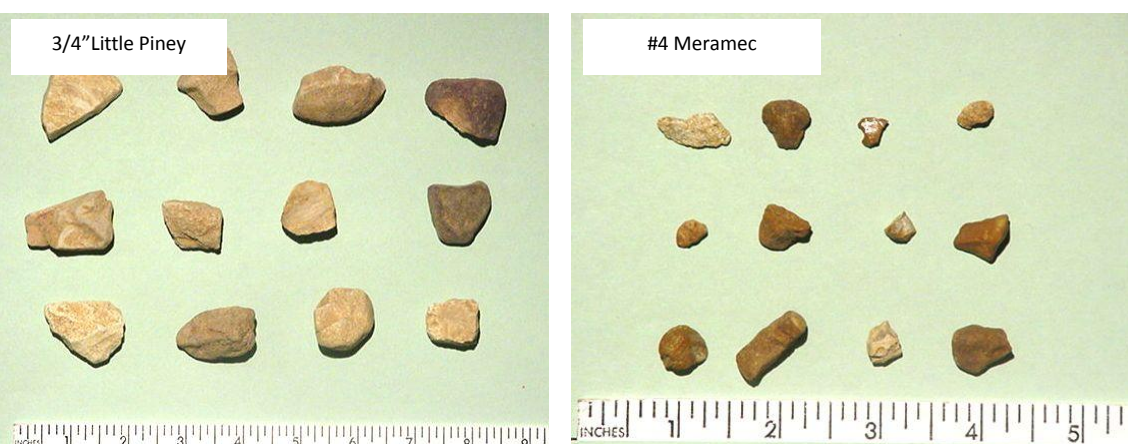


Figure C.7. Meramec River Aggregate

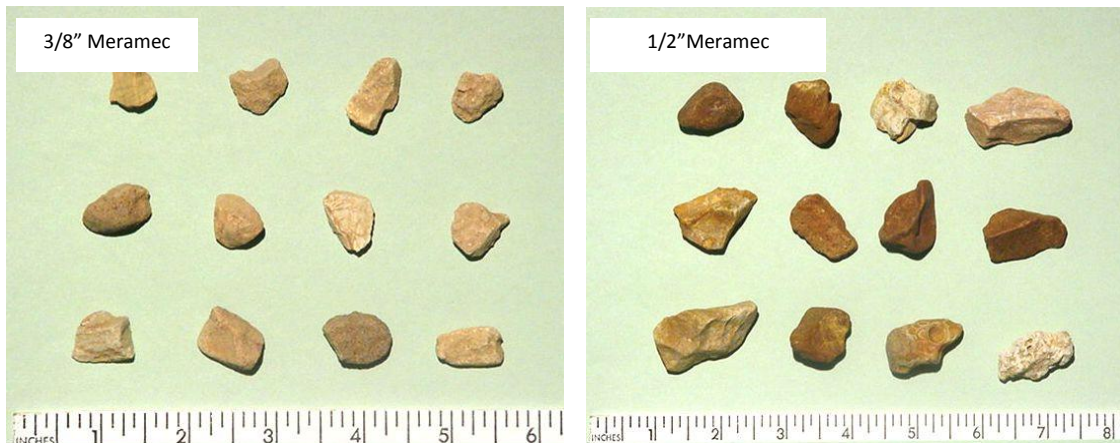


Figure C.8. Meramec River and Missouri River Aggregate



Figure C.9. Missouri River Aggregate

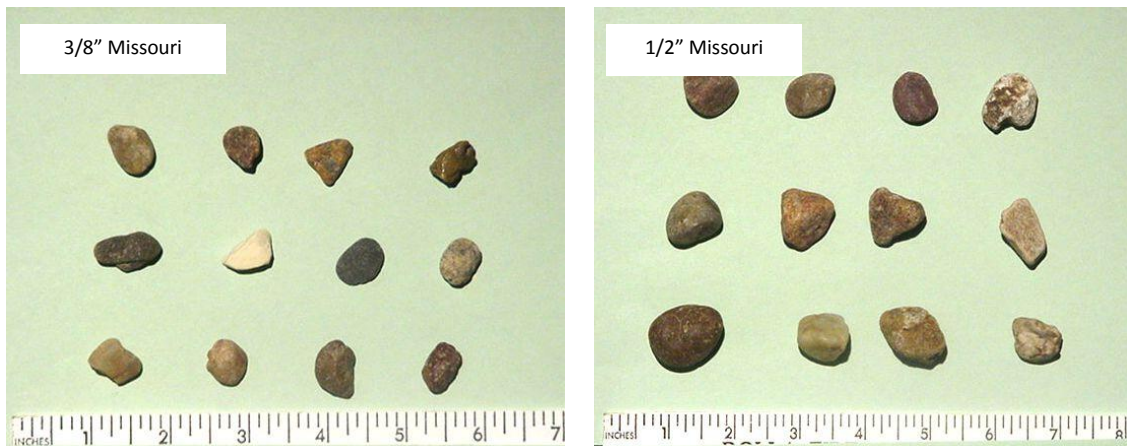


Figure C.10. Osage River Aggregate



BIBLIOGRAPHY

American Association of State Highway and Transportation Officials (AASHTO). (1999). "Standard Test Method for Uncompacted Void Content of Coarse Aggregate." TP56-99, Washington, D.C.

American Association of State Highway and Transportation Officials (AASHTO). (1999). "Specific Gravity and Absorption of Coarse Aggregate." No. T 85, Washington, D.C.

American Concrete Institute (ACI). (1999). "Aggregates for Concrete." *ACI Education Bulletin E1-99*, Committee E-701, Farmington Hills, MI, 17-18.

American Society for Testing and Materials (ASTM). (2000c). "Standard Practice for Conducting an Interlaboratory Test Program to Determine the Precision of Test Methods for Construction Materials." *ASTM Designation C 802-96*, Philadelphia, PA.

American Society for Testing and Materials (ASTM). (2000a). "Standard Test Method for Index of Aggregate Particle Shape and Texture." *ASTM Designation D 3398-00*, Philadelphia, PA.

American Society for Testing and Materials (ASTM). (2000b). "Standard Test Method for Uncompacted Void Content of Fine Aggregate." *ASTM Designation C 1252-00*, Philadelphia, PA.

American Society for Testing and Materials (ASTM). (2001a). "Standard Test Method for Determining the Percentage of Fractured Particles in Coarse Aggregate." *ASTM Designation D 5821-01*, Philadelphia, PA.

American Society for Testing and Materials (ASTM). (2001b). "Standard Test Method for Density, Relative Density (Specific Gravity), and Absorption of Coarse Aggregate." *ASTM Designation C 127-01*, Philadelphia, PA.

American Society for Testing and Materials (ASTM). (1998). "Standard Practice for Reducing Samples of Aggregate to Testing Size." *ASTM Designation C 702-98*, Philadelphia, PA.

Asphalt Institute (1996). *Superpave Mix Design, Superpave Series No. 2*, Lexington, Kentucky, 3-5.

Barksdale, R. D., Kemp, M. A., Sheffield, W. J., and Hubbard, J. L. (1991). "Measurement of Aggregate Shape, Surface Area, and Roughness." *Transportation Research Record 1301*, Transportation Research Board, Washington, D.C., 107-116.

Barrett, P. J. (1980). "The Shape of Rock Particles, A Critical Review." *Sedimentology*, 27, 291-303.

Benson, F. J. (1968). "Effects of Aggregate Size, Shape, and Surface Texture on the Properties of Bituminous Mixtures-A Literature Survey." *Highway Research Board, Special Report 109*, Washington D.C., 12-22.

Britton, W. S. G. (1968). "Effects of Aggregate Size, Shape, and Surface Texture on the Durability of Bituminous Mixtures." *Highway Research Board, Special Report 109*, Washington D.C., 23-24.

Browne, C., Rauch, F. A., Haas, T. C., and Kim, H. (2001). "Comparison Tests of Automated Equipment for Analyzing Aggregate Gradation." *Proceedings of the 9th Annual Symposium of the International Center for Aggregate Research (ICAR)*, Austin, TX.

Brzezicki, J. M., and Kasperkiewicz, J. (1999). "Automatic Image Analysis in Evaluation of Aggregate Shape." *Journal of Computing in Civil Engineering*, Vol. 13, No. 2, 123-128.

Buchanan, S. M. (2000). "Evaluation of the Effect of Flat and Elongated Particles on the Performance of Hot Mix Asphalt Mixtures." *NCAT Report*, No. 2000-3.

D'Angelo, J. A. (1996). "Superpave and Aggregate Properties: Where Did They Come From and Where Are They Going." *Proceedings of the Center for Aggregates Research, 4th Annual Symposium*, 1-10.

Fletcher, T., Chandan, C., Masad, E., and Sivakumar, K. (2002). "Measurement of Aggregate Texture and Its Influence on HMA Permanent Deformation." *Journal of Testing and Evaluation, American Society for Testing and Materials, ASTM*, Vol. 30, No. 6, 524-531.

Franklin, J. A. (1996a). "Fragment Shape Measurement in Geology and Other Fields – Applications to Blasting." *Proceedings of the FRAGBLAST 5 Workshop on Measurement of Blast Fragmentation*, Montreal, Canada, 33-38.

Franklin, J. A. (1996b). "Appendix 3. Classified Bibliography on Measurement of Fragmentation, Image Analysis and Related Topics." *Proceedings of the FRAGBLAST 5 Workshop on Measurement of Blast Fragmentation*, Montreal, Canada, 283-314.

Frost, J. D., and Lai, J.S. (1996). "Digital Analysis of Aggregate Particle Shape." *Proceedings of the Center for Aggregates Research, Fourth Annual Symposium*, Atlanta, GA.

Janoo, V. C. (1998). "Quantification of Shape, Angularity, and Surface Texture of Base Course Materials." *Cold Regions Research and Engineering Laboratory, Special Report 98-1*, 22 pp.

Kalcheff, I. V., and Tunnicliff, D. G. (1982). "Effects of Crushed Stone Aggregate Size and Shape on Properties of Asphalt Concrete." *Association of Asphalt Paving Technologists*, Vol. 51, 453-483.

Kim, H., Hass, C., Rauch, A., and Browne, C. (2001). "A Prototype Laser Scanner for Characterizing Size and Shape Properties in Aggregates." Proceedings of the 9th Annual Symposium of the International Center for Aggregate Research (ICAR), Austin, TX.

Kim, H., Haas, C. T., Rauch, A. F., and Browne, C. (2002). "Wavelet-Based 3D Descriptors of Aggregate Particles." *Transportation Research Record 1787*, Transportation Research Board, National Research Council, Washington, D.C., 109-116.

Krumbein, W. C. (1940). "Flood Gravels of San Gabriel Canyon, California." *Geol. Soc. America Bull.*, v. 11, 639-676.

Krumbein, W. C., and Sloss, L. L. (1951). *Stratigraphy and Sedimentation*, W. H. Freeman, San Francisco, CA., 497 pp.

Kuo, C. Y., Frost, J. D., Lai, J. S., and Wang, L. B. (1996). "Three-Dimensional Image Analysis of Aggregate Particles from Orthogonal Projections." *Transportation Research Record, Issue 1526*, Transportation Research Board, Washington, D.C., 98-103.

Kuo, C., Rollings, R. S., and Lynch, L. N. (1998). "Morphological Study of Coarse Aggregates Using Image Analysis." *Journal of Materials in Civil Engineering*, Vol. 10, 135-142.

Maerz, N. H., (1998). "Aggregate Sizing and Shape Determination Using Digital Image Processing." *Center For Aggregates Research (ICAR) Sixth Annual Symposium Proceedings*, St. Louis, MO., 195-203.

Maerz, N. H., and Zhou, W. (1999). "Flat and Elongated: Advances Using Digital Image Analysis." *Center for Aggregates Research (ICAR) Seventh Annual Symposium Proceedings*, Austin, TX., B1-4-1 to B1-4-12.

Maerz, N. H., and Lusher, M. (2001). "Measurement of Flat and Elongation of Coarse Aggregate Using Digital Image Processing." *Proceedings of the Transportation Research Board, 80th Annual Meeting*, Washington D.C., Paper No. 01-0177.

- Mandel, J. (1971). "Repeatability and reproducibility." *In: Materials Research and Standards, American Society of Testing and Materials (ASTM)*, 8-15.
- Masad, E., Button, J. W., and Papagiannakis, T. (2000). "Fine-Aggregate Angularity, Automated Image Analysis Approach." *Transportation Research Record 1721*, Transportation Research Board, Washington D.C., paper no. 00-0691, 66-72.
- Masad, E., Olcott, D., White, T., and Tashman, L. (2001). "Correlation of Imaging Shape Indices of Fine Aggregate with Asphalt Mixture Performance." *Proceedings of the Transportation Research Board, 80th Annual Meeting, 2001*, Washington D.C., Paper No. 012123, 25 pp.
- Masad, E. (2003). "The Development of a Computer Controlled Image Analysis System for Measuring Aggregate Shape Properties." *National Cooperative Highway Research Program NCHRP-IDEA Project 77 Final Report*, Transportation Research Board, National Research Council, Washington, D.C.
- National Cooperative Highway Research Program (NCHRP) (2003). "Aggregate Tests for Portland Cement Concrete Pavements: Review and Recommendations." *Research Results Digest, No. 281*, Transportation Research Board, National Research Council, Washington, D.C., 7-15.
- National Stone, Sand and Gravel Association. (1991). *The Aggregate Handbook*.
- Pettijohn, F. J. (1949). *Sedimentary Rocks*, Harper & Row, New York.
- Prowell, B. D., and Weingart, R. (1999). "Precision of Flat and Elongated Particle Tests: ASTM 4791 and VDG-40 Videograder." *Proceedings of the Transportation Research Board, 78th Annual Meeting*, Washington D.C.
- Rao, C., Tutumluer, E. (2000). "A New Image Analysis Approach for Determination of Volumes of Aggregates." *Proceedings of the Transportation Research Board, 79th Annual Meeting*, Washington D.C., Paper No. 001345, 25 pp.
- Rao, C., Tutumluer, E. and Kim, I. T. (2002). "Quantification of Coarse Aggregate Angularity Based on Image Analysis." *Transportation Research Record 1787*, Transportation Research Board, National Research Council, Washington, D.C., 117-124.
- Rao, C., Pan, T., and Tutumluer, E. (2003). "Determination of Coarse Aggregate Surface Texture Using Image Analysis." *16th ASCE Engineering Mechanics Conference, University of Washington, Seattle, WA*.

Smith, M. R., and Collis. L. (2001). "Aggregates: Sand, Gravel, and Crushed Rock Aggregates for Construction Purposes, 3rd Edition." *Geological Society Engineering Geology Special Publication No. 17*, London Geological Society, London.

Tutumluer, E., Rao, C., and Stefanski, J. (1999). "Progress Report for Video Analysis of Aggregates." *Federal Highway Administration*.

Tyler, W. S. (2001), "Particle Size and Shape Analyzers (CPA)." *Product Brochure*, Mentor, OH.

Wadell, H. (1932). "Volume, Shape and Roundness of Rock Particles." *Journal of Geology*, 40, 443-451.

Weingart, R. L., and Prowell, B. D. (1998/1999) "Flat and Elongated Aggregate Tests: Can the VDG-40 Videograder Deliver the Needed Precision for Particle Shape and Determination and be Economically Viable?" *Stone Review*, 20-23.

VITA

Gregory Allen Swift was born in Springfield, Missouri on February 17, 1971. His family settled in Tulsa, Oklahoma in 1984, after residing in three different states. Swift graduated from Bixby High School, just outside of Tulsa, in 1989 and began his collegiate career at Southwest Missouri State University. After two semesters at SMSU, Swift transferred to the University of Missouri-Rolla in 1990. He spent two semesters at Rolla and was unsure if he wanted to pursue a career in engineering. He worked several different jobs until joining the United States Marine Corps in 1993. While serving in the Marine Corps, Swift was stationed at Camp Pendleton, California and also performed the duties of a Marine Security Guard at United States Embassies in Copenhagen, Denmark and Dakar, Senegal where he attained the rank of sergeant.

Swift returned to Rolla in 1998 to continue his pursuit of an engineering degree, while continuing to serve in the Marine Corps Reserves. He received a Bachelor of Science degree in Geological Engineering from the University of Missouri-Rolla in May of 2001 and a Master of Science degree in Geological Engineering from the University of Missouri-Rolla in December of 2007.